HHS Public Access

Author manuscript

*Ocul Surf*. Author manuscript; available in PMC 2024 October 01.

Published in final edited form as:

*Ocul Surf*. 2023 October ; 30: 17–41. doi:10.1016/j.jtos.2023.07.012.

# The miR-183/96/182 Cluster Is a Checkpoint for Resident Immune Cells and Shapes the Cellular Landscape of the Cornea

**Weifeng Li**[1,2], **Katherine Gurdziel**[3], **Ahalya Pitchaikannu**[4], **Naman Gupta**[4], **Linda D. Hazlett**[4], **Shunbin Xu**[4,*]

[1]Predoctoral Training Program in Human Genetics, McKusick-Nathans Institute of Genetic Medicine, Department of Genetic Medicine

[2]Wilmer Eye Institute, School of Medicine, The Johns Hopkins University, Baltimore, Maryland

[3]Genome Sciences Core, Visual and Anatomical Sciences, School of Medicine; Wayne State University, Detroit, Michigan

[4]Department of Ophthalmology, Visual and Anatomical Sciences, School of Medicine; Wayne State University, Detroit, Michigan

## Abstract

**Purpose:** The conserved miR-183/96/182 cluster (miR-183C) regulates both corneal sensory innervation and corneal resident immune cells (CRICs). This study is to uncover its role in CRICs and in shaping the corneal cellular landscape at a single-cell (sc) level.

**Methods:** Corneas of naïve, young adult [2 and 6 months old (mo)], female miR-183C knockout (KO) mice and wild-type (WT) littermates were harvested and dissociated into single cells. Dead cells were removed using a Dead Cell Removal kit. CD45+ CRICs were enriched by Magnetic Activated Cell Sorting (MACS). scRNA libraries were constructed and sequenced followed by comprehensive bioinformatic analyses.

**Results:** The composition of major cell types of the cornea stays relatively stable in WT mice from 2 to 6 mo, however the compositions of subtypes of corneal cells shift with age. Inactivation of miR-183C disrupts the stability of the major cell-type composition and age-related transcriptomic shifts of subtypes of corneal cells. The diversity of CRICs is enhanced with age. Naïve mouse cornea contains previously-unrecognized resident fibrocytes and neutrophils. Resident macrophages (ResMϕ) adopt cornea-specific function by expressing abundant extracellular matrix (ECM) and ECM organization-related genes. Naïve cornea is endowed with partially-differentiated proliferative ResMϕ and contains microglia-like Mϕ.

*Correspondence: Shunbin Xu, Department of Ophthalmology, Visual and Anatomical Sciences, School of Medicine Wayne State University, 540 E Canfield Street, Detroit, MI48201. Telephone: 313-577-0127. Fax: 313-577-3125. sxu@med.wayne.edu.



Disclosure/Conflict of Interest Statement

The authors declare no conflict of interest.

Resident lymphocytes, including innate lymphoid cells (ILCs), NKT and γδT cells, are the major source of innate IL-17a. miR-183C limits the diversity and polarity of ResMϕ.

**Conclusion:** miR-183C serves as a checkpoint for CRICs and imposes a global regulation of the cellular landscape of the cornea.

### Keywords

single cell RNA sequencing (scRNA seq); microRNAs (miRNAs); miR 183/96/182 cluster (miR-183C); Corneal resident immune cells (CRICs); resident macrophages (ResMϕ); corneal resident fibrocytes (CRFs); corneal resident myeloid cells (CRMCs); corneal resident lymphocytes (CRL); corneal resident neutrophils (CRNs)

## Introduction

The cornea is the interface between the eye and the external environment. It is avascular and transparent to allow visual clarity and provide two thirds of the refractive power of the eye[1–3]. It is also the first-line defensive barrier against microbial invasion and other insults[1–3]. Multiple cell types from different tissue origins contribute to the cellular composition of the cornea. They work in concert to maintain homeostasis and meet functions of the cornea. These include surface ectoderm-derived corneal epithelium, neural crest-derived stromal keratocytes and endothelial cells as well as corneal nerves, and mesoderm-derived corneal resident immune cells (CRICs)[1–3]. During development, different cellular components join the cornea in a tightly controlled manner. In the mouse, the specification of corneal epithelium (CEpi) starts at ~ embryonic day (E)8.5[4, 5], when the lens placode is specified by the induction of the optic vesicle[1, 6]. As the lens placode invaginates to form the lens pit, and the lens vesicle detaches from the surface ectoderm (~E11.5)[5], mesenchymal cells migrate into the space between the lens and newly specified CEpi to form the corneal stroma (CSL) and the endothelial layer (CEndoL. ~E14.5–15.5) [1, 2]. Meanwhile, tissue resident macrophages (ResMϕ) from the early erythromyeloid progenitors (EMP) of the yolk sac integrate into the corneal region as early as E9.0[7], the late EMP of fetal liver at ~E11.5–16.5 and definitive hematopoietic stem cells (HSCs) of the bone marrow at ~E17.5 and after birth[7, 8]. Sensory nerves from the trigeminal ganglia (TG) begin to project into the cornea starting as early as E12.5[9, 10]; however, the anatomy of the corneal nerves does not reach maturity until postnatal 8 weeks old[11]. These different cell types form the microenvironment or niche and interact with one another to maintain the homeostasis of the cornea, keeping it transparent under physiological conditions and mounting defense responses in the event of microbial invasion and tissue damage.

Multiple types of CRICs have been reported in the cornea, e.g., Langerhans cells (LCs) [12–14] and γδ T cells in the CEpi layer[15–19], and monocytes (MCs)/Mϕ[12, 20] and dendritic cells (DCs) in the CSL[12, 13, 21]. CRICs play important roles in normal development and homeostasis of the cornea, including: ocular immune privilege, transplant graft survival, wound healing, corneal nerve regeneration, innate immune/inflammatory responses to tissue damage and microbial infection and orchestration of adaptive immune responses[15–28]. However, the CRICs are a rare population in the cornea, accounting for approximately1.2 – 5% of total corneal cells in the mouse cornea[8, 29, 30]. Despite their

importance, our understanding of CRICs, including their accurate numbers and relative representations in the cornea, their molecular signatures and classification, mechanisms underlying their functions and interactions with other cell types to shape the corneal cellular landscape, remains limited.

In this regard, single-cell RNA sequencing (scRNA seq) has become a powerful tool to study the transcriptomes of individual cells and dissect the molecular complexity of a tissue. Comparing to other tissues/organ systems, e.g. the retina[31–33], brain[34–36], and immune system [37–39], fewer scRNA seq studies have been done in the cornea. When we began this project, there were only three publications of scRNA seq in the cornea[40–42]. Two of these reports focused on limbal stem cells (LSCs) and did not detect any CRICs[40, 42]. The other report focused on nonmyelinated Schwann cells in the CSL of rabbit cornea[41]. Although ~34 cells (out of 6,546) were identified as “tissue-resident macrophages and dendritic cells”[41], no additional characterization was done; and no additional types of CRICs detected[41]. Recently, more scRNA seq studies on mouse and human corneas have been reported. However, most of these studies still focus on LSCs[43–46]. One report described molecular characterization of human corneal immune cell types; however, the source of the cells was from the limbal region only[47]. Collins et al. reported a single-cell atlas of human cornea and adjacent conjunctiva and identified two clusters of immune cells, including MC-derived Mϕ and DCs, two types of CD8+ T cells and Mϕ[48]. However, the focus of this report was on other corneal cell types; no further analysis on the immune cells was performed; it was unclear whether these immune cells are derived from the cornea or adjacent conjunctiva[48]. Wieghofer et al.[7] reported scRNA seq of fluorescence activated cell sorting (FACS)-purified myeloid cells ($CD45^{+}CD3^{-}CD19^{-}Ly6G^{-}$) from the cornea, retina and ciliary body of young adult mice. Although this report provided new insights into molecular characteristics and classification of myeloid cells in these different compartments of the eye, to date, there is still no complete molecular characterization and catalog of CRICs at a single-cell level.

microRNAs (miRNAs) are newly recognized, small, non-coding RNAs and are important post-transcriptional regulators of gene expression[49–52]. They play important roles in human diseases[53] and are viable therapeutic targets[54]. However, their roles in CRICs and the homeostasis of the cornea are still unknown. Recently, we and others identified that a conserved, paralogous miRNA cluster, the miR-183/96/182 cluster (referred to as miR-183C from here on), regulates the functions of both primary sensory neurons of all major sensory domains[55–61] and innate immune cells[30, 62–66]. In the cornea, inactivation of miR-183C results in decreased nerve density and a disrupted pattern of the subbasal plexus with reduced levels of neuropeptides and pain receptor molecules[64]. In innate immune cells, miR-183C regulates the production of proinflammatory cytokines and their phagocytosis and bacterial killing capacity[30, 64, 65]. Recently, we discovered that miR-183C regulates the number of CRICs under homeostatic conditions; inactivation of miR-183C leads to increased number of CRICs, including ResMϕ[30]. These data suggest that miR-183C has dual regulation of both corneal sensory innervation and CRICs. We, therefore, hypothesize that, through these regulations, miR-183C plays an important role in modulating the cellular composition and the homeostasis of the cornea.

To test this hypothesis and to achieve a complete molecular characterization and classification of CRICs in the context of the entire cornea, we performed scRNA-seq in total corneal cells and CD45+ MACS-enriched corneal cells of 2 and 6 months old (mo) miR-183C knockout (KO) and their age- and sex-matched wild-type control (WT) mice. Here we report our data which provide an in-depth molecular characterization and catalog of CRICs and the roles of miR-183C in shaping the corneal cellular landscape.

## Materials and Methods

### Mice.

Naïve, young adult (2 and 6 mo), female miR-183C KO, miR-183C$^{GT/GT}$, and their age- and sex-matched WT control mice on a 129S2-C57BL/6-mixed background[56] were used for scRNA sequencing. All experiments and procedures involving animals and their care were pre-reviewed and approved by the Wayne State University Institutional Animal Care and Use Committee and carried out in accordance with National Institutes of Health and Association for Research in Vision and Ophthalmology guidelines.

### Single cell RNA sequencing.

Adult mouse corneas anterior to the limbus were harvested and dissociated into single cells by enzymatic digestion with collagenase A (MilliporeSigma. Cat No. 10103578001) and DNase I (MilliporeSigma. Cat No. 11284932001) in Hanks' Balanced Salt solution (HBSS) and trituration as we described previously[30]. For the total corneal cell preparation, corneas from 3 mice/genotype/age were pooled as one biological sample. Dead cells were removed using the Dead Cell Removal Microbeads and Magnetic Activated Cell Sorting (MACS) column (Miltenyi Biotech). Live single cells were subjected to sc cDNA library production using the Chromium Next GEM Single Cell 3' Reagent kit v3.1 and the Chromium Controller (10xGENOMICS) following the manufacturer's instructions. On average, we obtained ~128,715 [±10,757 Standard Error of the Mean (SEM)] single cells/cornea after the enzymatic and mechanical dissociation [Supplemental table 1 (Table S1)].

To enrich for CRICs, corneas of 7 KO or 8 WT naïve, 6 mo mice were pooled as one biological sample. After dead cell removal, CD45+ (a pan-leukocyte marker) cells were enriched using the anti-CD45 microbeads and MACS (Miltenyi Biotech) following the manufacturer's instructions, before sc cDNA library construction.

Subsequently, the sc cDNA libraries were sequenced on a NovaSeq sequencer (Illumina) at the Genome Sciences Core (GSC), Wayne State University (WSU).

### scRNA seq data analysis.

Reads were aligned to the mouse genome (Build mm10) using *Cell Ranger$^{TM}$ v6.0.1* (10xGenomics). The filtering criteria for QC include a minimum of 30 cells/gene and 500 features/cell and percentage of mitochondrial genes <10%. The basic characteristics of the scRNA seq data for the total corneal cells and CD45+ MACS-enriched cells are summarized in Tables S2&S3 and Supplemental Figures (Fig.S).1 & 2. Cell populations were identified by unbiased clustering based on normalized gene expression values using Principal

Component Analysis (PCA) dimensional reduction and embedded in two dimensions using Uniformed Manifold Approximation and Projection (UMAP) analysis in *Seurat* 4.0.6[67] on *R*4.1.2.

Major cellular identities of the clusters were first assigned based on the expression of known cell type-specific marker genes and further refined by the unbiased cell-identity analysis software *SingleR/Celldex*[68]. Signature genes (SigGenes) for each population/cluster and differentially expressed genes (DEG) between KO and WT samples were identified using *Seurat* function FindAllMarkers or FindMarkers. miR-183C target prediction in the DEG or SigGenes were performed using TargetScan[69, 70]. Prediction of molecular pathways and biological processes in which the SigGenes or DEGs are involved were analyzed using Database for Annotation, Visualization and Integrated Discovery (DAVID)[71], Gene Ontology enRIchment anaLysis and visuaLizAtion tool (Gorilla)[72] and Reduce+Visualize Gene Ontology (Revigo)[73] as described before[74].

## Results

### 1. miR-183C modulates corneal cellular composition and age-related changes

We obtained 26,125 sc transcriptomes from total corneal cell samples, including 6,915 and 6,526 cells of 2 mo WT and miR-183C KO mice; 7,402 and 5,282 corneal cells of 6 mo WT and KO mice, respectively (Table 1). Unbiased clustering analyses identified 20 different cell cluster/populations based on their sc transcriptomes (Fig.1A; Table S4).

Cell type identification by known cell type-specific markers identified that eight clusters, including Clusters 4,7,10,11,13,15,16 and 17, represent various subtypes of corneal epithelial cells (CEpiCs) because of their collective expression of mouse CEpiC marker, Krt12 [75](Fig.1B&L) and many other epithelial cell markers expressed in CEpiCs, including Pax6, Cdh1, Krt6b (Fig.1C–E), Krt5, Krt6a, Krt7, Krt13, Krt14, Krt15, Krt80, Cldn4, Muc1, Muc4, and Muc20[75–86] (Fig.S3.B–O). Conjunctival epithelium-specific Krt19[87] is barely expressed (Fig.S3P).

The conglomerate of eleven clusters, including Clusters 0,1,2,3,5,6,8,9,14,18 and 19, contained subtypes of corneal stromal keratocytes (CSKCs) because of their predominant expression of CSKC markers, Keratocan (Kera), Lumican (Lum) and Vimentin (Vim) (Fig.1F,G&L; Fig.S4). Corneal endothelial cell (CEndoC)-specific markers, aquaporin 1 (Aqp1)[88, 89], NCAM1[90], Zo-1(Tjp1) and Alcam[91] were also expressed in these clusters (Fig.1H&I; Fig.S5). Other endothelial cell markers, e.g. Atp1a1, Atp1b1, Atp1b2, Itga5, Col8a1, Slc3a2, Slc7a5, Cd248 were enriched in various subpopulations of these clusters (Fig.S6), suggesting that this 11-cluster conglomerate represents both CSKCs and CEndoCs, consistent with their common neural crest origins.

Cluster 12 clearly represents CRICs because of its specific expression of pan-leukocyte marker, CD45 (Ptprc) (Fig.1J), myeloid specific markers Csf1r (Fig.1K,L), Lyz2, Fcgr1 (CD64), Fcer1g, antigen-presenting and processing (APP) markers, Cd74, MHCII molecules, H2-Aa, H2-Ab1, immune adaptor molecule Tyrobp, and complement factors, C1qa, C1qb and C1qc (Fig.S7).

In WT mice, the overall corneal cellular landscape categorized by the major cell types of CEpiCs, CSKC/CEndoCs and CRICs showed only subtle changes between 2 and 6 mo (Fig.2A–C; Fig.S8A; Table 2; Table S5&S6), suggesting that the composition of major cell types is relatively stable in adult mouse cornea under homeostatic condition. On average, CEpiCs, CSKC/CEndoCs and CRICs account for approximately 25.86%, 72.58% and 1.56% of all corneal cells, respectively (Fig.2B&C;Table 2). However, several subpopulations of CEpiCs and CSKC/CEndoCs manifested >1.5-fold changes between 2 and 6 mo WT mice. In CEpiCs, Clusters 7 and 15 were decreased by 2.39 and 4.07 folds, respectively; while Cluster 13 was increased by ~2.06 folds (Fig.2D; Fig.S8B; Table S6). Among subpopulations of CSKC/CEndoCs, 8 out of the 11 clusters showed >1.5-fold changes. Clusters 0, 2, 6 were decreased by ~3.60, 4.42, and 3.17 folds, respectively; while Clusters 1, 5, 8 were increased by ~2.83, 12.06 and 35.63 folds, respectively (Fig.2D; Fig.S8B; Table S6). Cluster 9, which was undetected in 2 mo, accounted for 0.08% in 6 mo WT cornea (Table S6); while Cluster 19, which accounted for 0.30% at 2 mo, was undetected at 6 mo in WT cornea. These data suggest that, in adult WT mice, although the representations of the major cell types are relatively stable, subtypes of corneal cells shift to cope with the adult life to maintain the homeostasis of the cornea.

In KO mice, the cellular landscape of major cell types of the cornea showed apparent changes from 2 to 6 mo (Fig.2A–C). CEpiCs, CSKC/CEndoCs and CRICs accounted for approximately 37.01%, 61.49% and 1.50% of total corneal cells at 2 mo; while 19.65%, 77.04% and 3.31% at 6 mo, respectively (Table 2; Fig.2B&C). CEpiCs were decreased by ~1.88 folds, while CSKC/CEndoCs and CRICs were increased by ~ 1.25 and 2.21 folds, respectively, in 6 vs 2 mo mice (Fig.2B&C; Table 2; Fig.S8C; Tables S5&S6). This result suggests that inactivation of miR-183C impacts the major cellular composition of the steady-state cornea.

In addition, six out of the 8 subtypes/clusters of CEpiCs showed >1.5-fold changes: Clusters 7, 10, 11, 15, and 16 were decreased by 3.66, 2.28, 2.42, 7.55 and 8.17 folds, respectively; while Cluster 17 was increased by 2.55 folds (Fig.2D; Fig.S8D, Table S6B), resulting in an overall decrease of CEpiCs in the corneas of 6 vs 2 mo KO mice. Among CSKC/CEndoCs, 8 clusters showed >1.5-fold changes: four, including Clusters 2, 3, 5, and 18, were decreased by 2.87, 4.87, 2.59 and 3.04 folds, respectively; while Clusters 0 and 8 were increased by 1.89 and 32.43 folds, respectively, in 6 vs 2 mo old mice (Fig.2D; Fig.S8D, Table S6). Clusters 9 and 19 were undetected in 2 mo, while accounted for 21.70% and 0.04% of total corneal cells, respectively, in 6 mo KO mice. These changes collectively led to a moderate overall increase of CSKC/CEndoCs in 6 vs 2 mo mice.

Comparing 2 mo WT vs KO mice, the overall representation of CEpiCs was increased by 1.36 folds in KO (37.01%) vs WT mice (27.22%) (Fig.2A&B; Fig.S8E; Table 2; Table S6). Among 8 CEpiC clusters, 3 clusters, Clusters 7, 10 and 16, were increased by 2.04, 1.80 and 1.95 folds, respectively, resulting in an overall slight increase of CEpiCs in the KO vs WT mice (Fig.2D; Fig.S8F; Table S6). For CSKC/CEndoCs, although their overall representation showed only a minor change between WT (71.11%) and KO mice (61.49%) (Table 2; Fig.S8E), 4 subpopulations/clusters of CSKC/CEndoCs (Clusters 0, 5, 18 and 19) had >1.5-fold changes (Fig.2D; Fig.S8F; Table S6): Clusters 0 and 5 were decreased by 2.15

and 1.50 folds, respectively, in KO vs WT mice; while Cluster 18 was increased by ~ 4 folds. Cluster 19 accounted for 0.30% of all corneal cells in WT mice, while undetected in 2 mo KO mice(Fig.2D; Fig.S8F; Tables S5&S6).

At 6 mo, although the overall representations of CEpiCs and CSKC/CEndoCs were similar between KO and WT mice (Table 2; Fig.2B&C; Fig.S8G; Table S6), many subtypes/clusters of CEpiCs and CSKC/CEndoCs showed >1.5-fold changes between KO and WT mice. CEpiC clusters 10, 11, 13, and 16 were decreased by 1.59, 1.50, 1.96 and 5.64 folds in KO vs WT mice, respectively (Fig.2D; Fig.S8H; Table S6). Among CSKC/CEndoC, seven clusters, including Clusters 0, 1, 3, 5, 6, 9 and 19, showed >1.5-fold changes in KO vs WT mice (Fig.2D; Fig.S8H; Table S6): Clusters 1, 3 and 5 were decreased by 2.07, 3.41, and 46.99 folds; while Clusters 0, 6, and 9 were increased by 3.16, 3.65 and 267.66 folds, in the KO vs WT mice, respectively. Cluster 19 was not detected in the WT mice, while accounted for 0.04% in the KO mice (Fig.2D; Fig.S8H; Table S6). For CRICs, although its overall representation was similar between KO (1.50%) and WT mice (1.68%) at 2 mo, CRICs were increased by 2.29 folds in KO (3.31%) compared to WT mice (1.45%) at 6 mo (Fig.2D; Fig.S8H; Table S6), suggesting miR-183C regulates the number of CRICs in naïve adult mouse cornea, which is consistent with our previous report[30].

## 2. miR-183C regulates the composition and transcriptomes of corneal resident immune cells

CRICs are a rare population in the cornea[8, 29, 30]. Although we obtained an average of 6,531 sc transcriptomes (5282 – 7402) from total corneal cells (Table 1), only ~124 CRICs (98 −175) were captured, accounting for approximately 1.98% (1.45%−3.31%) of total corneal cells (Tables S5B&S6B). To enhance the number of CRICs, we enriched CRICs from 6 mo miR-183C KO and WT control mice using MACS with anti-CD45 microbeads for scRNA seq. From these CD45+ MACS-enriched corneal cells, we obtained a total of 3254 sc transcriptomes, including 1089 and 2165 from WT and KO mice, respectively (Table 3).

Unbiased clustering identified four major populations (Fig.S9). Manual cell type identification by known cell type-specific markers showed that Cluster 0 represents the CRICs because of their specific expression of CD45 (Ptprc), and myeloid cell markers, Csf1r and Fcgr1 (Fig.S9C–E), and many other immune cell markers (data not shown). Cluster 1 represents CSKCs and CEndoCs (Fig.S9F–I); Cluster 2&3 CEpiCs (Fig.S9J–T). Conjunctival epithelial cell-specific marker Krt19 was not detected (Fig.S9U), consistent with the fact that the source of the cells was the cornea anterior to the limbus region. In the CD45+ MACS-enriched corneal cells, CRICs accounted for 35.2% and 54.1% in WT and KO mice, respectively, suggesting a 24- and 16-fold enrichment of CRICs (Table S7C), when compared to their frequencies in the total corneal cells of 6 mo mice (Fig.2C; Fig.S8G; Table S6B).

To maximize the number of CRIC transcriptomes for downstream comprehensive analyses, we pooled the sc transcriptomes of the CRICs from the total corneal cells and the CD45+MACS enriched cells to obtain a total of 2044 CRIC sc transcriptomes (Table

4; Fig.S10; Table S8). Unbiased clustering analysis of the pooled CRICs identified 10 populations/subtypes of CRICs, Clusters 0–9 (Fig.3A; Fig.S10).

In WT mice, although the overall representation of CRICs in total corneal cells showed little change from 2 to 6 mo (Fig.2C), the composition of CRICs displayed global changes (Fig.3B–E; Fig.S11A&B; Table S9). Relative representations of seven clusters showed >1.5-fold changes. Clusters 1, 6 and 9 were decreased by 2.48, 1.98 and 2.79 folds, respectively; while Clusters 2 and 5 were increased by 6.10 and 3.23 folds; Clusters 7 and 8 were undetected at 2 mo, but accounted from 2.86% and 4.02%, respectively, in 6 mo mice (Fig.S11A&B; Table S9D).

Inactivation of miR-183C resulted in drastic changes of the cellular landscape of CRICs (Fig.3B–E). At 2 mo, relative representations of four clusters (Clusters 2, 5, 6 and 7) showed >1.5-fold changes. Cluster 2 was increased by 1.55 folds in KO mice. Cluster 7 was undetected in WT mice, however, accounted for 2.06% of CRICs in KO mice. Clusters 6 were decreased by 1.72 folds; while Cluster 5 was decreased from 0.88% in WT to undetectable in KO mice (Fig.3B&C; Table S9D).

At 6 mo, the differences of CRIC compositions between KO and WT mice were further enhanced. Relative representations of nine out of 10 clusters had >1.5-fold changes (Fig.3D&E). Among these, Clusters 0, 1, 2 and 4 were decreased by 6.88, 2.49, 1.66 and 6.63 folds (Fig.3D&E; Table S9D). Clusters 5, 7, 8 and 9 were increased by 4.22, 1.61, 4.22 and 1.81 folds in KO vs WT mice, respectively. Cluster 3 was undetected in WT mice, but accounted for 44.83% of all CRICs in 6 mo KO mice (Fig.3D&E; Table S9D), underscoring a major impact of miR-183C on CRIC transcriptomes.

Transcriptome analyses identified a series of SigGenes for all clusters/subtypes of CRICs (Fig.4A; Tables S10–S12). Manual cell-type identification with known immune cell markers identified two major categories of CRICs. The majority (95.6%, Clusters 0–6,8,9) expressed myeloid cell markers, Csf1r, Fcgr1 (CD64), Itgam (Cd11b) and Lyz2, suggesting their corneal resident myeloid cell (CRMC) identity (Fig.4B–F; Table S9A). T lymphocyte markers, Cd3d, Cd3e, Cd3g, and CD3ζ, were exclusively expressed in Cluster 7, suggesting that Cluster 7, which accounts for 4.4% of CRICs, represents the corneal resident lymphocyte (CRL) population (Fig.4G–K; Table S9A).

### 3. miR-183C regulates the functional differentiation of CRMCs

To further dissect the identity of the CRMCs in the cornea, we first analyzed known markers for MCs, Mϕ and DCs. Several key MC markers, including Ly6C, CD62L (encoded by Sell),CD43 (encoded by Spn)[92] were not detected (Table S10). Other key MC-associated markers, including Ccr2 and Cx3cr1[92] (Fig.5A–C; Table S10) were expressed at a relatively low level in most myeloid clusters, with Cluster 2 having the highest percentage of Ccr2+ cells (Table S10&S13). Known Mϕ markers, including Adgre1 (F4/80), Mertk, Mrc1, Ms4a7, Fcrls and Pf4 (Fig.5D–J) were recognized in all the myeloid cell clusters. These data suggest that MCs which migrate into the cornea quickly downregulate their MC signature genes and differentiate into Mϕ with various transcriptomic signatures.

Previously, various DC populations, including Langerhans cells, have been described in the cornea[12, 13, 93]. However, in the transcriptomes of CRICs of naïve mouse cornea, most major known DC and Langerhans cell markers and associated genes were undetected. These include Itgax (Cd11c), CD209 (DC-SIGN), Cd103, Sirpa (Cd172), Irf4, Flt3, Ly75, Ccr7, Ccl22, Kmo, Zbt46, Clec9a, Cd207 (Langerin) and Cd1a[36, 94–96] (Table S10).

To further delineate the identities of CRMCs, we performed unbiased cell-type recognition using the Single Cell-Recognition (SingleR) software [68] in association with the Immunological Genome Project database (ImmGenData)[97]. The ImmGenData, consisted of microarray profiles of pure mouse immune cells from the Immunological Genome Project (http://www.immgen.org)[97], is the most comprehensive and highly resolved immune reference database. Consistent with the result by manual identification using known cell type-specific markers (Figs.4&5), SingleR analysis confirmed that the vast majority [up to 87.28% (1784 out of 2044)] of all pooled CRICs are Mϕ (Fig.6A; Table 5; Table S14A). The representations of Mϕ in CRICs stayed relatively stable (between 70–80%) in both WT and KO mice at both 2 and 6 mo (Table S14C). Their representations in the total corneal cells of WT mice also stayed stable from 2 to 6 mo (~1.13%); however, in the KO mice, the relative representation of ResMϕ was increased from 1.2% to ~2.4% in 2 and 6 mo KO mice, respectively (Table S14C). This contributed to the increased overall representation of CRICs in total corneal cells in 6 mo KO mice (Tables S6).

Similar to our manual cell-type identification result, SingleR/ImmGenData analysis identified only a small fraction of CRICs as MCs (1.27%, or 26 out of 2044 of all CRICs), which were predominantly distributed in Clusters 2 (65.4% of all MCs)(Fig.6B; Table 5; Table S14A), consistent with the observation of the highest percentage of Ccr2+ cells in Cluster 2 (Fig.5A,C; Tables S10&S13). An even smaller fraction (0.78%, or 16 out of 2044 of all CRICs) was recognized as DCs (Fig.6C; Table 5; Table S14A), which were also predominantly (~93.8%, or 15/16) distributed in Cluster 2, in close vicinity to the MCs (Fig.6B&C; Table 5; Table S14A). These data suggest that Cluster 2 may represent the newly arrived MCs from which most of the other types of myeloid cells are derived in the corneal niche. Consistent with this hypothesis, a single-cell trajectory analysis using publicly available *Monocle 2* software[98] placed Cluster 2 in the center of the trajectory tree, suggesting divergent directions and/or states of differentiation towards other myeloid clusters (Fig.6F).

Analysis of the original sources of these MCs and DCs showed that both were derived from 6 mo mice, but not detected from 2 mo mice (Table S14C). In 6 mo WT mice, both MCs and DCs accounted for 0.95% of all CRICs or 0.01% of all corneal cells (Table S14C), suggesting enhanced diversity of CRICs with age. In 6 mo KO mice, the numbers of MCs and DCs were increased and accounted for 5.17% and 3.45% of CRICs or 0.17% and 0.06% of all corneal cells, respectively (Table S14C), suggesting that miR-183C limits the number of MCs and DCs in the homeostatic cornea.

Analysis of the transcriptomes of the Mϕ, DCs and MCs in Cluster 2 identified a series of signature genes of these myeloid cells in this cluster (Fig.6E; Table S15). Consistent with their identities of Mϕ or DCs, Gene Ontology (GO) analysis showed that the Cluster-2 Mϕ

were signified by the expression of effector molecules involved in complement activation (C1qa, C1qb, C1qc), leukocyte chemotaxis (Cxcl2 and Pf4), and regulation of innate immune responses (ApoE and Treme2); while DC signature genes are most enriched with genes involved in APP, e.g. MHCII molecule H2-DMb2 and TAP1, and adaptive immune response and immune system process, e.g. Msfsd6, Tap1, Jmal, and H2-DMb2 (Table S15).

**3.1. miR-183C regulates the differentiation of APP ResMϕ—**Although the naïve cornea has few DCs (Fig.6C), corneal ResMϕ are endowed with different expression levels of APP-related genes. Cluster 0 showed the highest expression of APP-related genes (Fig.7A–C; Table S10–12). GO term and Kyoto Encyclopedia of Genes and Genomes (KEGG) pathway analyses showed that SigGenes of Cluster 0 were overwhelmingly enriched with genes involved in APP signaling pathways, e.g. MHCII molecules, H2-Aa, H2-Ab1, H2-Eb1, Cd74 (Fig.7A–C; Tables S16&S17). Following Cluster 0, Clusters 1, 2, 4 and 9 manifested gradually decreased levels of APP marker expression (Fig.7A–C), suggesting a possible gradual differentiation to APP Mϕ from the MCs in Cluster 2 (Fig.6F–a). Cluster 7, consistent with their lymphocyte identity, showed little APP gene expression (Fig.7A–C).

The representations of clusters with highest expression levels of APP genes, including Clusters 0, 1, 2 and 4, were drastically decreased by approximately 6.88, 2.49, 1.66 and 6.63 folds, respectively, in the KO vs WT control mice at 6 mo, although their representations were at similar levels at 2 mo (Fig.3; Table S9). This result suggests that miR-183C positively regulates the differentiation towards APP ResMϕ; when miR-183C is inactivated, APP ResMϕ differentiation is inhibited. Since miRNAs regulate their downstream genes in a quantitative manner, this inhibitory effect accumulates with age, resulting in profound changes by 6 mo.

**3.2. Inactivation of miR-183C results in the emergence of a subpopulation of ResMϕ signified of enhanced potentiation of M2 polarity.—**While the representation of APP ResMϕ declined in 6 mo KO mice, a subpopulation of corneal ResMϕ unique to the KO mice emerged – Cluster 3 (Fig.3; Table S9). Functional annotation analysis showed that key genes involved in metabolic pathways were significantly enriched in the SigGenes of Cluster 3 (Tables S11,S12,S18&S19). Metabolic status is known to play a central role in Mϕ polarity and functions. M1-polarized Mϕ mainly engage in aerobic glycolysis even under normoxic conditions [99, 100], and HIF-1 is a major driver of glycolytic gene expression [99, 100]; while M2 polarization depends on a fully functional tricarboxylic acid (TCA) cycle and oxidative phosphorylation (OXPHOS) activity, although an intact glycolytic pathway is also required to feed into the TCA cycle [99, 100]. The most striking feature of Cluster 3 was that one of the most prominent hallmark genes of alternative immune response or M2 polarization, Arginase (Arg)1, was its No.1 SigGene (Fig.8A&B; Tables S11&S12). In addition, other genes important for M2 polarity, e.g. genes involved in OXPHOS pathways, e.g. Cox5a/b, Cox6a1/b1/c, Atp5b/e/g1, Atp6v0b/0e/1f/1g1, Cycs, Uqcrq, Uqcrb, etc, were also significantly enriched (Table S19). Consistently, GO analysis showed significant enrichment of GO terms of mitochondrial electron transport and cell redox homeostasis (Tables S20&S21). These data suggest ResMϕ of Cluster 3 are

metabolically highly active and are potentiated toward M2 polarity. Intriguingly, key genes involved in M1 polarization-related pathways, such as glycolysis, carbon metabolism, HIF-1 signaling pathway, e.g. Aldoa, PKM, Gapdh, Eno1, Tpi1, Ldha, PGK1, were also highly enriched in the SigGenes of Cluster 3 (Fig.8A&B; Tables S18–21), suggesting a potential M1/M2 hybrid polarity[101–103]. These data collectively indicate that miR-183C limits the extent of the potentiation of M2 and/or M1/M2 hybrid polarities; inactivation of miR-183C enhances the differentiation toward M2 and/or M1/M2 hybrid polarities.

### 3.3. Corneal ResMϕ are reprogrammed to adopt corneal specific functions by expressing genes important for extracellular matrix (ECM) production and organization.—

In addition to metabolism-related genes, many genes encoding key ECM components, ECM organization and cell-ECM interaction regulators, e.g., Vim[104], Galectin-3 (Lgals3)[105, 106], Tgfβ-induced gene (Tgfbi, also known as βig-h3 and keratoepithelin)[107–109], fibronectin (Fn1)[110], secreted phosphoprotein 1 [Spp1, also known as osteopontin (Opn)][111–114] and fatty acid-binding protein 5 [Fabp5, also known as Fabp-epidermal (E-Fabp)][115, 116], were also enriched in Cluster 3 (Fig.8C–E; Tables S10–12). Furthermore, SigGenes of Cluster 3 also included cytokines regulating cellular interaction with ECM and chemotaxis, e.g. Ccl6, Ccl9, platelet factor 4 (Pf4, also known as Cxcl4) and Cxcl14 (Fig.8C–D; Tables S10–12). Although the expression level was the highest in Cluster 3, these ECM-related genes were also expressed in the other ResMϕ clusters. Their expressions in Cluster-3 Mϕ were comparable to, some were even higher than, the ones in CSKC/CEndoC and/or CEpiCs (Fig.8E; Tables S4&S10). ECM is a major component of the cornea and plays essential roles in keeping the structure, transparency and other functions of the cornea[3, 108]. These data suggest that corneal ResMϕ adopt tissue-specific functions to contribute to ECM production and organization, and hence, the basic structure and functions of the cornea.

### 3.4. Naïve cornea is endowed with resident fibrocytes; miR-183C regulates the size of this population.—

The transcriptome of Cluster 6 was highlighted with SigGenes of both myeloid cells, e.g. Csf1r, Itgam (Cd11b) and Lyz2 (Fig.4) as well as fibroblasts (Fig.9; Tables S11&S12). Genes encoding the major components of corneal stromal ECM, e.g., Col1a1, Col1a2, Col5a1, Col12a1, and genes regulating ECM organization, e.g., keratan sulfate proteoglycan (KSPG) family members, Kera and Lum[1, 3], small leucine-rich proteoglycan, Decorin (Dcn)[117, 118] and alpha2-macroglobulin (A2M)[119] were among the top SigGenes of Cluster 6 (Fig.9A&B; Tables S11&S12). Many other collagen genes are also enriched the SigGenes of Cluster 6, including Col4a1, Col5a2, Col6a1/2/3, Col7a1, Col8a2, Col11a1, Col13a1, Col16a1, and Col23a1 (Tables S10&S11). Another prominent feature of Cluster 6 was its highly, specific expression of a hematopoietic stem marker, Cd34 (Fig.9A&B). Therefore, cells in Cluster 6 carried all the hallmarks of fibrocytes - simultaneous expression of hematopoietic markers, CD45 and CD34, and collagens[120–123]. Hence, we identified Cluster 6 represents previously unidentified corneal resident fibrocytes (CRFs) at homeostatic state. The “fibroblasts”, “stromal cells” and “Mϕ” identified by SingleR in Cluster 6 (Table S14) are possibly subtypes of CRFs. That SingleR analysis using the ImmGenData failed to recognize CRFs is a result of lack of the fibrocyte category in the ImmGenData[97].

Tgfβ pathways are known to play important roles in corneal development, corneal stromal ECM production and organization, fibrosis and wound healing[124, 125] as well as in fibrocyte function[126, 127]. Consistent with the fibrocyte identity, Tgfβ2 is highly enriched in Cluster 6 (Fig.9A&B). GO analysis confirmed that SigGenes of Cluster 6 were enriched with genes involved in collagen fibril organization, collagen biosynthetic process, ECM organization, cell migration and wound healing (Table S22). Functional pathway analysis of the SigGenes of Cluster 6 identified significant enrichment of ECM-receptor interaction pathways (Fig.9C; Table S23).

At 2 mo, Cluster-6 CRFs accounted for 28.3% and 16.5% of CRICs (Fig.9D), and 0.46% and 0.25% of total corneal cells of WT and KO mice, respectively (Fig.9E; Table S9D). This frequency of CRFs in the cornea is within the range of fibrocyte frequency in circulating non-erythrocytes of peripheral blood[120, 128]. Considering that on average mouse cornea contains at least 128,715 cells/cornea (Table S1), we estimate that there are approximately 596 and 321 CRFs per cornea in 2-mo WT and KO mice, respectively (Fig.9F). This data suggests that inactivation of miR-183C resulted in a decreased number of CRFs in the cornea of KO vs WT mice at 2 mo. However, at 6 mo, Cluster-6 CRFs accounted for 14.3% and 13.22% of CRICs (Fig.9D), and ~0.2% and 0.44% of all corneal cells of WT and KO mice, respectively (Fig.9E; Table S9D), which estimates ~257 and 566 CRFs per cornea of WT and KO, respectively (Fig.9F; Table S9D). These data indicate that from 2 mo to 6 mo, the number of CRFs per cornea was decreased (by ~56.6%) in WT mice, while increased (by ~76%) in KO mice; suggesting miR-183C regulates the size of the CRF population in steady-state cornea and has different effects at different ages.

GO and KEGG pathway analyses both revealed that SigGenes of Cluster 6 were also enriched with clock genes regulating the circadian rhythm pathway, e.g. Clock, Bhlhe40, Bhlhe41, Nr1d1, Per3, and Rora (Fig.S14; Tables S22&S23), suggesting that CRFs in the cornea may function with a circadian rhythm to cope with corneal ECM maintenance in a 24-hour cycle.

### 3.5. Mouse corneas are endowed with resident neutrophils; miR-183C modulates the number of corneal resident neutrophils (CRNs)—

Cluster 8 was only detected in the cornea of 6 mo, but not 2 mo mice (Table S9D). SigGene analysis revealed that Cluster 8 was highlighted by pro-inflammatory cytokine and receptor genes, e.g. Il1b, Il1r2, Cxcr2, Csf3r, S100a8, S100a9, Ptgs2, Mmp9, Clec4e, Ifitm1, suggesting enrichment of Mϕ with pro-inflammatory M1 polarity (Fig.10A&B; Tables S11&S12). Consistently, GO analysis revealed significant enrichment of pro-inflammatory GO terms, e.g., response to lipopolysaccharide, leukocyte migration involved in inflammatory response, positive regulation of nitric oxide biosynthetic process, positive and negative regulation of the inflammatory response (Fig.10C; Table S24). However, GO analysis also revealed enrichment of important neutrophil-related biological functions, e.g. neutrophil chemotaxis, positive regulation of neutrophil degranulation (Fig.10C; Table S24). In accordance, KEGG pathway analysis identified that SigGenes of Cluster 8 were enriched in neutrophil extracellular trap (NET) formation, leukocyte transendothelial migration and NOD-like receptor signaling pathways (Fig.10D; Table S25), suggesting that Cluster 8 may contain neutrophils.

Consistent with this prediction, unbiased cell type identification using SingleR/ImmGenData of Cluster 8 cells revealed that it indeed contained two major populations: neutrophils (55.7%. 34/61) and Mϕ (41.0%. 25/61) (Fig.11). SigGenes of the neutrophils in Cluster 8 were enriched with genes involved in neutrophil functions, e.g. neutrophil chemotaxis, neutrophil aggregation, and inflammatory responses (Fig.11C; Tables S27&S28); while the Mϕ in Cluster 8 were predominantly enriched with genes involved in APP and modulation of adaptive immune responses (Fig.11C; Table S29). Comparison of the transcriptomes of the neutrophils and Mϕ of Cluster 8 (Table S30) with other CRIC clusters revealed that, the expression levels of pro-inflammatory cytokines and related molecules in Cluster-8 Mϕ were much higher than all other CRIC clusters (Fig.S15; Table S31), suggesting that Cluster 8 contained ResMϕ, which are potentiated towards pro-inflammatory M1 polarity.

Analysis of the source of the Cluster 8 cells revealed that they were only detected in the corneas of 6 mo but not in 2 mo mice (Tables S9&S26). At 6 mo, the M1-potentiated Mϕ were only identified in the KO, but not WT mice (Table S26); the neutrophils were increased in the KO (3.4%) vs WT control mice (1.0% of CRICs)(Table S26). This result suggests that the diversity of CRICs is enhanced by age; miR-183C limits the potentiation of corneal ResMϕ towards the pro-inflammatory M1 polarity and the number of CRNs in naïve adult cornea.

### 3.6. Adult mouse cornea contains proliferative differentiated Mϕ; inactivation of miR-183C expands this population—

Cluster 9 is a subpopulation of corneal ResMϕ (Figs.4–7; Table S14). Consistent with this, the top 100 genes of Cluster 9 were significantly enriched with APP and immune response-related GO terms (Table S32). Intriguingly, SigGenes of Cluster 9 were almost exclusively enriched with cellular proliferation-related GO terms (Table S33). Similarly, Reactome pathway analysis[129] showed prominent enrichment of cell cycle-related pathways (Table S34).

Ki67 is a proliferative cell marker expressed in all stages of a cell cycle except the G0 phase[130]. Consistent with the bioinformatic findings, Ki67 was highly enriched in the Mϕ of Cluster 9 (Fig.12A&B). 47.1% of the cells in Cluster 9 expressed Ki67, which accounted for approximately 32.7% of all Ki67+ CRICs (Table S35A). This result suggests that adult mouse cornea is endowed with proliferative Mϕ under homeostatic condition, which are predominantly represented in Cluster 9.

Comparing WT and KO mice, the total number of Ki67+ CRICs were increased in the KO mice (2.63%) vs WT mice (1.83% of all CRICs)(Fig.12C; Table S35B). In Cluster 9, KO mice also showed a higher percentage Ki67+ cells in Cluster 9 (55.0%) when compared to the WT mice (35.7%)(Table S35B), suggesting that miR-183C limits CRIC proliferation; inactivation of miR-183C enhanced the proliferation of CRICs in the homeostatic cornea.

Mϕ expressing APP markers, e.g. Cd74, MHCII genes H2-Aa, H2-Ab1, H2-Eb1, are considered differentiated and functionally matured Mϕ. Intriguingly, all Mki67+ cells in Cluster 9 co-expressed one or more APP markers (Table S36; Figs.7&12). The majority [87.5% (14/16)] of Mki67+ cells co-expressed all four APP markers. These data suggest that proliferative Mϕ in naïve mouse corneas are differentiated, if not fully mature Mϕ, which

may provide a potential mechanism for the cornea to timely replenish functional Mϕ to meet their constant surveillance duty.

**3.7. Adult mouse cornea contains microglia (MG)-like resident Mϕ—**Unbiased cell type identification by SingleR/ImmGenData [68, 97, 131] recognized 12 MG in the pooled CRICs (~0.59%), which were distributed in Mϕ Clusters 0 (n=3), 1 (n=4), 4 (n=1), 5 (n=3) and 9 (n=1) (Table S14). We identified a series of SigGenes of microglia-like cells in the cornea (Table S37), the top 10 of which Ssna1, Smchd1, Prdx4, Ppfia4, Lsm8, Ankrd49, Stxbp2, Nde1, Siva1 and Ube2g2.

At 2 mo, the MG-like Mϕ, distributed in Clusters 0 and 9, accounted for 2.65% (3/113) of all CRICs, or 0.043% of all corneal cells in WT mice(Table S38); while in KO mice, 1.03% (1/97) of CRICs (in Cluster 0) or 0.015% (1/6526) of all corneal cells were identified as MG-like Mϕ (Table S38). Considering that, on average, 128,715 cells/cornea were isolated (Table S1), we estimated ~56 and 20 MG-like Mϕ/cornea of WT and KO mice, respectively (Table S38). At 6 mo, no MG was detected in the CRICs in WT mice; while only 1 MG (in Cluster 5) was detected in KO mice, accounting for ~0.57% (1/174) of CRICs or 0.019% of all corneal cells (Table S38). These data suggest that, from 2 to 6 mo, the number of MG-like Mϕ was decreased in the cornea of WT mice, but stayed stable in KO mice, although their transcriptomes shifted from 2 to 6 mo.

## 4. miR-183C regulates corneal resident lymphocytes, including innate lymphoid cells (ILCs), NKT cells and γδT cells.

As described above, Cluster 7 CRICs represent CRLs (Fig. 4;Table S39). KEGG pathway analysis of the SigGenes of Cluster 7 revealed significant enrichment with genes in the T cell receptor signaling pathway (Fig.S16; Table S40). Comparing KO vs WT mice, the relative representation of Cluster 7 in CRICs was consistently increased in the KO vs WT mice at both 2 mo (undetected in WT; 2.06% in KO mice) and 6 mo (2.86% in WT; 4.60% in KO mice)(Fig.3; Fig.S11; Table S9D), suggesting that miR-183C limits the number of CRLs in naïve mouse cornea.

The second most enriched pathway of Cluster 7 SigGenes is the Th17 cell differentiation pathway (Fig.13C; Table S40). Congruently, IL-17a and its transactivator, Rorc were among the prominent SigGenes of Cluster 7 (Fig.13A&B). IL-17a was expressed in 38.9% (35 of 90) of Cluster 7 cells, which accounted for >85% (35 out of 41) of all IL-17a-producing CRICs in the cornea (Table S41), suggesting that CRLs are the major source of innate IL-17-producing cells in naïve mouse cornea.

To further dissect the cellular identities of the CRLs in Cluster 7, we performed unbiased cell type identification using SingleR/ImmGenData. The result showed that Cluster 7 was a heterogenous population (Fig.14; Fig.S17). The majority of Cluster 7 cells were identified as ILCs (n=46; 51.1% of Cluster 7 cells), followed by NKT cells (n=29; 32.2%) and γδT cells (n=4; 4.4%)(Fig.14; Fig.S17). In addition, SingleR also identified Mϕ (n=7; 7.8%) and one of each of DC, NK and T cells (~1.1% of Cluster 7 cells) (Fig.14; Fig.S17). Among these different cell types, 37% of ILCs, 44.8% of NKT, 25% of γδT and 57.1% of Mϕ of Cluster 7 express IL-17a (Table S42), suggesting the existence of IL-17-produing

ILC3, NKT17, γδT17, and innate IL-17-producing Mϕ in naïve mouse cornea. Unbiased re-clustering of Cluster 7 cells did not further improve the segregation pattern of different cell types(Fig.14B; Fig.S17A), possibly reflecting the intrinsic similarities among these different innate lymphocyte populations[132–140]. Congruently, transcriptomic analysis of the SingleR-identified cell types of Cluster 7 revealed fewer SigGenes distinguishing the ILCs, NKT and γδT cells (Fig.S17B; Tables S43&S44).

Analysis of the sources of CRLs of Cluster 7 (Table S45B) showed that, for ILCs, at 2 mo, none was detected in the total corneal cell sample of WT mice; while 2 ILCs were detected in KO corneas, which accounted for ~2.06% (2/97) of CRICs and ~0.031% (2/6526) of total corneal cells]. Considering that, on average, mouse cornea contains at least 128,715 cells/cornea (Table S1), it estimated ~39 ILCs/cornea of KO mice at 2 mo (Table S45B).

At 6 mo, 2 ILCs were detected in WT cornea, accounting for ~1.90% (2/105) of CRICs or ~0.027% (2/7402) of total corneal cells, which estimates ~35 ILCs/cornea of 6-mo WT mice. In the 6-mo KO mice, 7 ILCs were detected, which accounted for ~4.02% (7/174) of CRICs or 0.13% (7/5282) of total corneal cells and an estimate of 171 ILCs/cornea of 6 mo KO mice (Table S45B). These data suggest that the numbers of ILCs were increased in 6 vs 2 mo of both WT and KO mice; and were increased in the KO vs WT mice at both ages. Data from the CD45+ MACS enriched CRICs corroborated with the observation on ILCs from the total corneal samples (Table S45B).

NKT cells are rarer than ILCs in the cornea. In the total corneal cell samples, they were too few to be detected in either WT or KO mice at 2 mo; while only 1 was detected in WT and KO mice at 6 mo (Table S45B). To gain any quantitative insight into the NKT population, we tapped into the data derived from the CD45+ MACS enriched CRICs, it showed that 0.26% (1/383) of CRICs were detected as NKT cells in the WT mice, while 2.22% (26/1172) of CRICs in the KO mice were identified as NKT cells (Table S45B). These data collectively suggest that NKT cells were also increased in 6 vs 2 mo mice regardless of their genotypes; inactivation of miR-183C resulted in an increased number of NKT cells in the cornea, at least at 6 mo.

None of the other cell types of Cluster 7, including γδT (n=4), were detected in the total corneal cell samples of either WT or KO mice at either 2 or 6 mo, suggesting their extreme rarity. They were only detected in the CD45+ MACS-enriched CRICs. For the γδT, they were only present in the MACS-enriched CRICs of the KO mice [~0.34% (4/1172)], but not in the ones from the WT mice (n=383), suggesting a potential increase of γδT in the cornea of 6-mo KO vs WT mice.

## Discussion

Based on >26,000 single-cell transcriptomes of total corneal cells, we established the first molecular classification and cellular catalog of steady-state mouse cornea at 2 and 6 mo. Our data provide an unprecedented body of new reference knowledge of mouse cornea, including the transcriptomes of all subtypes of CEpiCs, CSKC/CEndoC and CIRCs and the relative representations of all types and subtypes of corneal cells – the cellular

landscape of the cornea. In the past, using the traditional methodologies, e.g., histology, immunohistochemistry, immunofluorescence, FACS, etc, numerous pioneering studies have identified and quantified different cell types of the cornea based on their morphology and/or expression of specific marker genes. However, these studies characterized only one or several cell types at a time because of the limitations on the number of distinguishing markers, and therefore, can only obtain partial views of the corneal cellular biology. The systems biology approach of scRNA seq allows us to characterize, catalog and quantify all corneal cells at once based on their sc transcriptomes. Although several recent reports described scRNA seq studies of the cornea, these reports either focused on the limbal region and/or the adjacent conjunctiva [43–48], and therefore, cannot provide precise information of the cornea per se. In our study, the scRNA seq was performed on corneal cells of carefully dissected entire cornea anterior to the limbus; our data provide the first complete molecular catalog of the adult mouse cornea.

Comparison of the corneal cellular landscapes of 2 vs 6 mo WT mice, our data provide one of the first systems biology evidences that the cellular composition of adult cornea on a global scale is dynamic in nature. Although the cellular composition of the major cell types remained stable, the relative representations of many subtypes of all major cell types change from 2 to 6 mo, suggesting adaptative shift of corneal cellular landscape to cope with the increasing exposure of the environment to maintain the homeostasis of the cornea. We predict that under different environments, the corneal cellular transcriptomes and landscapes vary in response to different stimuli. Further study of the transcriptomic and cellular landscape changes under different environments, especially toxic environments, may provide new molecular mechanisms underlying the loss of homeostasis leading to the pathogenesis of environmental factor-related diseases, e.g. air pollution-associated dry-eye diseases[141, 142].

CRICs are known to play important roles in the normal development and functions of the cornea at its steady state and pathological conditions[15–28]. However, CRICs are a rare yet heterogenous population [8, 29, 30] and are embedded in the densely-packed corneal tissue. These factors have imposed major challenges to the studies on CRICs. Recently, several scRNA seq studies on CRICs have emerged. However, most of these reports dealt with the limbal region and/or included conjunctiva and other ocular tissues of human cornea [40–48, 143–145]; few detected substantial number of CRICs from mouse cornea. Some focused on FACS-sorted subpopulation of CRICs, e.g., CD45+CD3-CD19-Ly6G- myeloid cells from mouse cornea, ciliary body and retina[7], therefore, cannot provide molecular classification and catalog of all mouse CRICs and their relationships to other corneal cell types. Therefore, to-date, our knowledge on CRICs remains limited or fragmented; there still lacks a complete molecular classification and catalog of mouse CRICs. To fill this knowledge gap, we made CRICs the focus of the current study.

Based on, by far, the highest number of sc transcriptomes of mouse CRICs in one study (2044), this report provides the first in-depth molecular classification and catalog of CRICs of steady-state mouse corneas (Table 6). We identified 9 clusters of CRMCs, including at least 6 different cell types (Mϕ, MCs, DC, MG-like Mϕ, Fibrocytes, Neutrophils) and 1 cluster of CRLs, including at least three different cell types (ILCs, NKT and γδT cells). Our

data provide a new body of reference knowledge of CRICs, including the transcriptomes of all clusters and different types of CRICs and their relative representations in the cornea and their age-related changes in relation to other corneal cell types.

More importantly, we discovered several previously unrecognized new types of myeloid cells in naïve mouse cornea. First, although a very rare population in 6 mo WT mice (0.95% of CRICs), we identified that naïve mouse corneas are endowed with resident neutrophils. Neutrophils are the most abundant circulating leukocytes within the blood stream. For years, neutrophils are considered to be present exclusively in the circulation under physiological conditions. They infiltrate rapidly into tissues only after injury or infection, a process that is critical for the elimination of pathogens and tissue repair; while naïve tissues are free of these cells to be protected from their toxic cargo[146–149]. Recently, it has been shown that resident neutrophils are present in virtually all analyzed tissues under homeostatic condition, e.g., the lung, liver and spleen[147–154]. Tissue resident neutrophils are rapidly reprogrammed to acquire tissue-specific transcriptional signatures and non-canonical functional properties to support the physiological demands of their host tissues[154]. In the cornea, neutrophils are known to play a major role in corneal infectious diseases[155, 156]; however, resident neutrophils in naïve cornea have not been reported. Our finding of CRNs in naïve mouse cornea will have important implications to the understanding age-related differences in innate immunity of steady-state cornea, corneal response to microbial infection or injuries and considerations of different treatment strategies.

Second, fibrocytes are collagen-producing leukocytes[120, 122] and are considered to arise from circulating MC precursors[121, 122]. Fibrocytes play important roles in ECM production and organization, tissue remodeling, wound healing and fibrosis in diverse physiological and pathological settings[126, 127, 157–160]. Although infiltrating fibrocytes from the circulation have been reported in the cornea after phototherapeutic keratectomy (PTK)[127, 161] and in patients with Fuchs' dystrophy[162], CRFs have not been identified in naïve cornea. In this study, for the first time, we identified that CRFs exist in naïve mouse cornea at a frequency similar to the one of circulating non-erythrocytes of peripheral blood (0.1–0.5%) [120, 128]. Our finding of CRFs in naïve mouse cornea provides new insights into the basic corneal biology. CRFs may be a previously unidentified, important player in the maintenance of ECM production and organization, and therefore the normal architecture and transparency of steady-state cornea. The existence of CRFs also provides a plausible mechanism underlying the swift enhanced appearance of fibrocytes in damaged cornea, e.g. after PTK procedure[127, 161] and other corneal injuries.

In addition to the discovery of CRFs in steady-state cornea, we provide evidence that corneal ResMϕ are reprogrammed to support basic structure and functions of the cornea by expressing genes important for ECM construction and organization, e.g. Tgfbi, Vim, Lgals3/Galectin3, Fn1, Spp1/Opn and Fabp5 [107–112, 114–116, 163–168]. Collectively, these data suggest that CRMCs, including ResMϕ and CRFs, play important roles in ECM production and organization, and therefore, the maintenance of corneal basic architecture and function. Additional functional studies will be needed to confirm these hypotheses.

Innate lymphocytes, including ILCs, NKT cells and γδT cells, are enriched in mucosal tissues interfacing with the environment. They are innate counterparts of the adaptive immune system's helper T cells. Upon injury or microbial invasion, innate lymphocytes mount a swift inflammatory response independent of interactions with MHCII-presented antigens, bridging the innate and adaptive immune response [134, 135, 138, 140, 169–172]. Although ILCs[173–178], NKT cells[179–184] and γδT cells[18, 27, 185–192] have been described in the cornea and/or conjunctiva, all these reports described one type of the innate lymphocytes under various pathological conditions and mostly in the limbal region and/or conjunctiva. However, the status of CRLs in naïve mouse cornea is still unknown. In this report, we identified that a small fraction (<3%) of CRICs in the naïve mouse cornea are resident lymphocytes, including at least three types of innate lymphocytes, ILCs, NKT and γδT cells. Innate IL-17-producing cells are regarded as the sentinels of the immune system and are important in the maintenance of the mucosal barrier integrity under steady state, as well as pathological conditions[193–197]. Our data further revealed that CRLs are the major source of innate IL-17-producing cells in the cornea. All three subtypes of the CRLs produce IL-17a, suggesting the existence of IL-17-producing ILC3, NKT17 and γδT17 in steady-state cornea. To our knowledge, our report is the first in-depth molecular characterization of CRLs in naïve mouse cornea, suggesting that resident lymphocytes play a role in maintaining corneal homeostasis. Similar as other corneal cell types, the cellular landscapes of CRICs change with age, suggesting that age-related adaptation of CRICs to maintain the homeostasis of the cornea. Intriguingly, MCs, DCs and neutrophils (resident myeloid cells) and ILCs, NKT and γδT cells (innate lymphocytes) were only detected in the cornea of 6 mo, but not 2 mo WT mice. It is possible that these cell types may be too few to be detected in 2 mo corneas under the current experimental conditions. Nevertheless, these data suggest that the diversity of CRICs increases with age.

Previously, we have shown that, in the cornea, miR-183C is known to be specifically expressed in both the sensory nerves and CRICs[30, 64]; inactivation of miR-183C results in decreased corneal sensory nerve density and levels of neuropeptides[64] and increased number of CRICs and basal expression levels of both pro- and anti-inflammatory cytokines in the ResMϕ [30]. Our scRNA seq data in this study corroborate our previous findings of an overall increased number of CRICs in miR-183C KO mice[30]. Our data and revealed wide-spread changes of the relative representations of subtypes of CEpiC and CSKC/CEndoC in the miR-183C KO vs WT mice, suggesting that miR-183C KO-resulted changes in the corneal niche lead to transcriptomic shifts of subtypes of CEpiC and CSKC/CEndoC, an extrinsic function of miR-183C on corneal development. In CRICs, our data revealed enhanced numbers of MCs, DCs and neutrophils among CRMCs as well as all subtypes of CRLs in the KO vs WT mice. Furthermore, the numbers of proliferative CRICs (Ki67+) are also increased in KO vs WT mice. These data suggest that miR-183C regulates the number and diversity of CRICs in steady-state cornea, and that its regulation on the size of the CRIC population is, at least in part, through controlling their *in situ* proliferation in the cornea.

The effects of miR-183C on different types of CRICs appear to be highly cell-type specific. The most striking effect of miR-183C in CRICs is that inactivation of miR-183C led to the emergence of two subpopulations of ResMϕ, unique to miR-183C KO mice. The signature genes of these two subpopulations are enriched with either M1 (Mϕ in Cluster 8) or M2

(Cluster 3) markers, suggesting their potentiation towards either pro- or anti-inflammatory/pro-healing properties. Both subpopulations are undetected in 2 mo, but emerge in 6 mo mice exclusively (for Cluster 3) or predominantly (for Cluster 8) in KO mice. These data support a hypothesis that, under physiological condition, the cornea contains ResMϕ with potentials toward either M1 and/or M2 polarities to maintain its homeostasis and ensure its readiness to respond to various insults; miR-183C curtails the extent of their differentiation toward either end of the spectrum to moderate both pro- and anti-inflammatory functions. When miR-183C is inactivated, subpopulations towards both ends of the spectrum emerge. Since miRNAs' regulation of gene expression is quantitative in nature, it takes time to accumulate the effect, leading to the emergence of these subpopulations only in 6-mo mice. Collectively, our data suggest that miR-183C may serves as a cell type-specific checkpoint for CRICs. Further analyses of the difference between the sc transcriptomes of various types of CRICs of KO vs WT mice may identify cell type-specific targets of miR-183C underlying the mechanisms of its cell type-specific effects.

Our results show that, at the transcriptomic level, only a few MCs and DCs existed in the adult mouse cornea. This observation suggests that, once entering the cornea, MCs quickly downregulate their original signature genes and differentiate into Mϕ. Similar phenomena have been reported in other tissues. In liver, for example, MCs acquire Kupffer cell identity within hours after liver engraftment[198]. Our observation of few DCs in naïve mouse cornea is consistent with a recent report in central nervous system (CNS)[36]. However, it appears to be contradictory to other reports of various DC populations in the cornea[12, 13, 93]. This discrepancy may be due to the differences between expression levels of classical DC marker genes at transcriptional and protein levels and the differences of the methodologies. In the previous reports, identification of DCs by either FACS or immunostaining relied on the expression of specific cell markers, rather than their sc transcriptomes. Further investigations with a comprehensive panel of different approaches are needed to validate the representation of DCs in naïve mouse cornea.

Several limitations in the current study need to be addressed in future endeavors. First, despite unprecedented numbers of sc transcriptomes of total corneal cells were obtained, due to the rarity and diversity of CRICs, the number of several subpopulations of CRICs, e.g., the MCs, DCs, neutrophils and innate lymphocytes, remain too low for a reliable detection and thorough evaluation, especially in the 2 mo mice. For this reason, the relative representation of some of these cell types in the cornea may be skewed and need to be further validated. Second, since the major focus of this study is on CRICs and the global impact of age and miR-183C knockout on the cellular landscape of the cornea, we did not fully characterize all the subtypes of CEpiCs and CSKC/CEndoC. Major effort will be needed to further elucidate the functions of all subtypes of corneal cells in relation to their transcriptomes. Third, the results of this report are based on scRNA seq data, lacking further validation using other independent methods. For example, although we identified CRFs and CRNs, their localization and spatial distribution need to be confirmed by other methodologies, e.g. IHC and/or FACS. Furthermore, although numerous differences in percentage or number (or both) of these cell types were found between 2- and 6-mo mice or between WT and KO strains, many of these were small (<1 to 5%); the functional significance of these differences remains to be determined. The roles of newly identified

CRFs and CRNs in the development and homeostasis of the cornea need to be further defined.

In spite of these limitations, this study establishes the first in-depth molecular classification and cellular catalogs of mouse cornea and CRICs based on their sc transcriptomes. It identified age-related changes of corneal cellular composition and discovered previously unrecognized new types of CRICs and new transcriptomic features corneal ResMϕ indicative of cornea-specific functions. In addition, this study provides new insights into the roles of miR-183C in shaping the cellular landscape of the cornea. It also lays the foundation for systems-biology studies of the molecular mechanisms underlying corneal development and the pathogenesis of corneal diseases at a global scale and the development of informed therapy.

## Supplementary Material

Refer to Web version on PubMed Central for supplementary material.

## Acknowledgements

This research is supported by grants from the National Eye Institute, National Institutes of Health (R01 EY02605902 to SX; R01EY016058 and P30EY004068 to LDH), and by a Research to Prevent Blindness unrestricted grant to the Department of Ophthalmology, Visual and Anatomical Science, Wayne State University School of Medicine.

## References

[1]. Lwigale PY. Corneal Development: Different Cells from a Common Progenitor. Prog Mol Biol Transl Sci. 2015;134:43–59. [PubMed: 26310148]

[2]. Cvekl A, Tamm ER. Anterior eye development and ocular mesenchyme: new insights from mouse models and human diseases. Bioessays. 2004;26:374–86. [PubMed: 15057935]

[3]. DelMonte DW, Kim T. Anatomy and physiology of the cornea. J Cataract Refract Surg. 2011;37:588–98. [PubMed: 21333881]

[4]. Foster FS, Zhang M, Duckett AS, Cucevic V, Pavlin CJ. In vivo imaging of embryonic development in the mouse eye by ultrasound biomicroscopy. Invest Ophthalmol Vis Sci. 2003;44:2361–6. [PubMed: 12766031]

[5]. Lang RA. Pathways regulating lens induction in the mouse. Int J Dev Biol. 2004;48:783–91. [PubMed: 15558471]

[6]. Collomb E, Yang Y, Foriel S, Cadau S, Pearton DJ, Dhouailly D. The corneal epithelium and lens develop independently from a common pool of precursors. Dev Dyn. 2013;242:401–13. [PubMed: 23335276]

[7]. Wieghofer P, Hagemeyer N, Sankowski R, Schlecht A, Staszewski O, Amann L, et al. Mapping the origin and fate of myeloid cells in distinct compartments of the eye by single-cell profiling. EMBO J. 2021;40:e105123. [PubMed: 33555074]

[8]. Liu J, Xue Y, Dong D, Xiao C, Lin C, Wang H, et al. CCR2(−) and CCR2(+) corneal macrophages exhibit distinct characteristics and balance inflammatory responses after epithelial abrasion. Mucosal Immunol. 2017;10:1145–59. [PubMed: 28120849]

[9]. McKenna CC, Lwigale PY. Innervation of the mouse cornea during development. Invest Ophthalmol Vis Sci. 2011;52:30–5. [PubMed: 20811061]

[10]. McKenna CC, Munjaal RP, Lwigale PY. Distinct roles for neuropilin1 and neuropilin2 during mouse corneal innervation. PLoS One. 2012;7:e37175. [PubMed: 22615927]

[11]. He J, Bazan HE. Neuroanatomy and Neurochemistry of Mouse Cornea. Invest Ophthalmol Vis Sci. 2016;57:664–74. [PubMed: 26906155]

[12]. Hamrah P, Liu Y, Zhang Q, Dana MR. The corneal stroma is endowed with a significant number of resident dendritic cells. Invest Ophthalmol Vis Sci. 2003;44:581–9. [PubMed: 12556386]

[13]. Hattori T, Chauhan SK, Lee H, Ueno H, Dana R, Kaplan DH, et al. Characterization of Langerin-expressing dendritic cell subsets in the normal cornea. Invest Ophthalmol Vis Sci. 2011;52:4598–604. [PubMed: 21482644]

[14]. Lee EJ, Rosenbaum JT, Planck SR. Epifluorescence intravital microscopy of murine corneal dendritic cells. Invest Ophthalmol Vis Sci. 2010;51:2101–8. [PubMed: 20007837]

[15]. Li Z, Burns AR, Rumbaut RE, Smith CW. gamma delta T cells are necessary for platelet and neutrophil accumulation in limbal vessels and efficient epithelial repair after corneal abrasion. Am J Pathol. 2007;171:838–45. [PubMed: 17675580]

[16]. Li Z, Burns AR, Han L, Rumbaut RE, Smith CW. IL-17 and VEGF are necessary for efficient corneal nerve regeneration. Am J Pathol. 2011;178:1106–16. [PubMed: 21356362]

[17]. Byeseda SE, Burns AR, Dieffenbaugher S, Rumbaut RE, Smith CW, Li Z. ICAM-1 is necessary for epithelial recruitment of gammadelta T cells and efficient corneal wound healing. Am J Pathol. 2009;175:571–9. [PubMed: 19608878]

[18]. Li Z, Burns AR, Miller SB, Smith CW. CCL20, gammadelta T cells, and IL-22 in corneal epithelial healing. FASEB J. 2011;25:2659–68. [PubMed: 21518851]

[19]. Skelsey ME, Mellon J, Niederkorn JY. Gamma delta T cells are needed for ocular immune privilege and corneal graft survival. J Immunol. 2001;166:4327–33. [PubMed: 11254685]

[20]. Brissette-Storkus CS, Reynolds SM, Lepisto AJ, Hendricks RL. Identification of a novel macrophage population in the normal mouse corneal stroma. Invest Ophthalmol Vis Sci. 2002;43:2264–71. [PubMed: 12091426]

[21]. Knickelbein JE, Watkins SC, McMenamin PG, Hendricks RL. Stratification of Antigen-presenting Cells within the Normal Cornea. Ophthalmol Eye Dis. 2009;1:45–54. [PubMed: 20431695]

[22]. Niederkorn JY. Cornea: Window to Ocular Immunology. Curr Immunol Rev. 2011;7:328–35. [PubMed: 21789035]

[23]. Barabino S, Chen Y, Chauhan S, Dana R. Ocular surface immunity: homeostatic mechanisms and their disruption in dry eye disease. Prog Retin Eye Res. 2012;31:271–85. [PubMed: 22426080]

[24]. McClellan SA, Huang X, Barrett RP, van Rooijen N, Hazlett LD. Macrophages restrict Pseudomonas aeruginosa growth, regulate polymorphonuclear neutrophil influx, and balance pro- and anti-inflammatory cytokines in BALB/c mice. J Immunol. 2003;170:5219–27. [PubMed: 12734370]

[25]. Sarkar J, Chaudhary S, Jassim SH, Ozturk O, Chamon W, Ganesh B, et al. CD11b+GR1+ myeloid cells secrete NGF and promote trigeminal ganglion neurite growth: implications for corneal nerve regeneration. Invest Ophthalmol Vis Sci. 2013;54:5920–36. [PubMed: 23942970]

[26]. Foulsham W, Coco G, Amouzegar A, Chauhan SK, Dana R. When Clarity Is Crucial: Regulating Ocular Surface Immunity. Trends Immunol. 2018;39:288–301. [PubMed: 29248310]

[27]. Liu J, Li Z. Resident Innate Immune Cells in the Cornea. Frontiers in immunology. 2021;12:620284. [PubMed: 33717118]

[28]. de Paiva CS, St Leger AJ, Caspi RR. Mucosal immunology of the ocular surface. Mucosal Immunol. 2022;15:1143–57. [PubMed: 36002743]

[29]. Sosnova M, Bradl M, Forrester JV. CD34+ corneal stromal cells are bone marrow-derived and express hemopoietic stem cell markers. Stem Cells. 2005;23:507–15. [PubMed: 15790772]

[30]. Coku A, McClellan SA, Van Buren E, Back JB, Hazlett LD, Xu S. The miR-183/96/182 Cluster Regulates the Functions of Corneal Resident Macrophages. Immunohorizons. 2020;4:729–44. [PubMed: 33208381]

[31]. Macosko EZ, Basu A, Satija R, Nemesh J, Shekhar K, Goldman M, et al. Highly Parallel Genome-wide Expression Profiling of Individual Cells Using Nanoliter Droplets. Cell. 2015;161:1202–14. [PubMed: 26000488]

[32]. Shekhar K, Lapan SW, Whitney IE, Tran NM, Macosko EZ, Kowalczyk M, et al. Comprehensive Classification of Retinal Bipolar Neurons by Single-Cell Transcriptomics. Cell. 2016;166:1308–23 e30. [PubMed: 27565351]

[33]. O'Koren EG, Yu C, Klingeborn M, Wong AYW, Prigge CL, Mathew R, et al. Microglial Function Is Distinct in Different Anatomical Locations during Retinal Homeostasis and Degeneration. Immunity. 2019;50:723–37 e7. [PubMed: 30850344]

[34]. Mrdjen D, Pavlovic A, Hartmann FJ, Schreiner B, Utz SG, Leung BP, et al. High-Dimensional Single-Cell Mapping of Central Nervous System Immune Cells Reveals Distinct Myeloid Subsets in Health, Aging, and Disease. Immunity. 2018;48:599. [PubMed: 29562204]

[35]. Nowakowski TJ, Rani N, Golkaram M, Zhou HR, Alvarado B, Huch K, et al. Regulation of cell-type-specific transcriptomes by microRNA networks during human brain development. Nat Neurosci. 2018;21:1784–92. [PubMed: 30455455]

[36]. Jordao MJC, Sankowski R, Brendecke SM, Sagar, Locatelli G, Tai YH, et al. Single-cell profiling identifies myeloid cell subsets with distinct fates during neuroinflammation. Science. 2019;363.

[37]. Shalek AK, Satija R, Adiconis X, Gertner RS, Gaublomme JT, Raychowdhury R, et al. Single-cell transcriptomics reveals bimodality in expression and splicing in immune cells. Nature. 2013;498:236–40. [PubMed: 23685454]

[38]. Gaublomme JT, Yosef N, Lee Y, Gertner RS, Yang LV, Wu C, et al. Single-Cell Genomics Unveils Critical Regulators of Th17 Cell Pathogenicity. Cell. 2015;163:1400–12. [PubMed: 26607794]

[39]. Buenrostro JD, Corces MR, Lareau CA, Wu B, Schep AN, Aryee MJ, et al. Integrated Single-Cell Analysis Maps the Continuous Regulatory Landscape of Human Hematopoietic Differentiation. Cell. 2018;173:1535–48 e16. [PubMed: 29706549]

[40]. Kaplan N, Wang J, Wray B, Patel P, Yang W, Peng H, et al. Single-Cell RNA Transcriptome Helps Define the Limbal/Corneal Epithelial Stem/Early Transit Amplifying Cells and How Autophagy Affects This Population. Invest Ophthalmol Vis Sci. 2019;60:3570–83. [PubMed: 31419300]

[41]. Bargagna-Mohan P, Schultz G, Rheaume B, Trakhtenberg EF, Robson P, Pal-Ghosh S, et al. Corneal nonmyelinating Schwann cells illuminated by single-cell transcriptomics and visualized by protein biomarkers. J Neurosci Res. 2020.

[42]. Li DQ, Kim S, Li J, Gao Q, Choi J, Bian F, et al. Single-cell transcriptomics identifies limbal stem cell population and cell types mapping its differentiation trajectory in limbal basal epithelium of human cornea. The ocular surface. 2020.

[43]. Altshuler A, Amitai-Lange A, Tarazi N, Dey S, Strinkovsky L, Hadad-Porat S, et al. Discrete limbal epithelial stem cell populations mediate corneal homeostasis and wound healing. Cell Stem Cell. 2021;28:1248–61 e8. [PubMed: 33984282]

[44]. Dou S, Wang Q, Qi X, Zhang B, Jiang H, Chen S, et al. Molecular identity of human limbal heterogeneity involved in corneal homeostasis and privilege. The ocular surface. 2021;21:206–20. [PubMed: 33964410]

[45]. Li DQ, Kim S, Li JM, Gao Q, Choi J, Bian F, et al. Single-cell transcriptomics identifies limbal stem cell population and cell types mapping its differentiation trajectory in limbal basal epithelium of human cornea. The ocular surface. 2021;20:20–32. [PubMed: 33388438]

[46]. Li JM, Kim S, Zhang Y, Bian F, Hu J, Lu R, et al. Single-Cell Transcriptomics Identifies a Unique Entity and Signature Markers of Transit-Amplifying Cells in Human Corneal Limbus. Invest Ophthalmol Vis Sci. 2021;62:36.

[47]. Li Y, Jeong J, Song W. Molecular Characteristics and Distribution of Adult Human Corneal Immune Cell Types. Frontiers in immunology. 2022;13:798346. [PubMed: 35280984]

[48]. Collin J, Queen R, Zerti D, Bojic S, Dorgau B, Moyse N, et al. A single cell atlas of human cornea that defines its development, limbal progenitor cells and their interactions with the immune cells. The ocular surface. 2021.

[49]. Ambros V. The functions of animal microRNAs. Nature. 2004;431:350–5. [PubMed: 15372042]

[50]. Bartel DP. MicroRNAs: genomics, biogenesis, mechanism, and function. Cell. 2004;116:281–97. [PubMed: 14744438]

[51]. Wightman B, Ha I, Ruvkun G. Posttranscriptional regulation of the heterochronic gene lin-14 by lin-4 mediates temporal pattern formation in C. elegans. Cell. 1993;75:855–62. [PubMed: 8252622]

[52]. Lee RC, Feinbaum RL, Ambros V. The C. elegans heterochronic gene lin-4 encodes small RNAs with antisense complementarity to lin-14. Cell. 1993;75:843–54. [PubMed: 8252621]

[53]. Chang TC, Mendell JT. microRNAs in vertebrate physiology and human disease. Annu Rev Genomics Hum Genet. 2007;8:215–39. [PubMed: 17506656]

[54]. Jeyaseelan K, Herath WB, Armugam A. MicroRNAs as therapeutic targets in human diseases. Expert Opin Ther Targets. 2007;11:1119–29. [PubMed: 17665982]

[55]. Xu S, Witmer PD, Lumayag S, Kovacs B, Valle D. MicroRNA (miRNA) Transcriptome of Mouse Retina and Identification of a Sensory Organ-specific miRNA Cluster. J Biol Chem. 2007;282:25053–66. [PubMed: 17597072]

[56]. Lumayag S, Haldin CE, Corbett NJ, Wahlin KJ, Cowan C, Turturro S, et al. Inactivation of the microRNA-183/96/182 cluster results in syndromic retinal degeneration. Proc Natl Acad Sci U S A. 2013;110:E507–16. [PubMed: 23341629]

[57]. Busskamp V, Krol J, Nelidova D, Daum J, Szikra T, Tsuda B, et al. miRNAs 182 and 183 Are Necessary to Maintain Adult Cone Photoreceptor Outer Segments and Visual Function. Neuron. 2014.

[58]. Fan J, Jia L, Li Y, Ebrahim S, May-Simera H, Wood A, et al. Maturation arrest in early postnatal sensory receptors by deletion of the miR-183/96/182 cluster in mouse. Proc Natl Acad Sci U S A. 2017;114:E4271–E80. [PubMed: 28484004]

[59]. Lewis M, Quint E, Rzadzinska A, Kent-Taylor A, Fuchs H, Angelis MHD, et al. An ENU-induced mutation of a miRNA associated with progressive hearing loss. 6th Molecular Biology of Hearing and Deafness Conference. Wellcome Trust Conference Center, Hinxton, UK2007.

[60]. Mencia A, Modamio-Hoybjor S, Redshaw N, Morin M, Mayo-Merino F, Olavarrieta L, et al. Mutations in the seed region of human miR-96 are responsible for nonsyndromic progressive hearing loss. Nat Genet. 2009;41:609–13. [PubMed: 19363479]

[61]. Geng R, Furness DN, Muraleedharan CK, Zhang J, Dabdoub A, Lin V, et al. The microRNA-183/96/182 Cluster is Essential for Stereociliary Bundle Formation and Function of Cochlear Sensory Hair Cells. Scientific reports. 2018;8:18022. [PubMed: 30575790]

[62]. Donatelli SS, Zhou JM, Gilvary DL, Eksioglu EA, Chen X, Cress WD, et al. TGF-beta-inducible microRNA-183 silences tumor-associated natural killer cells. Proc Natl Acad Sci U S A. 2014;111:4203–8. [PubMed: 24586048]

[63]. Wurm AA, Zjablovskaja P, Kardosova M, Gerloff D, Brauer-Hartmann D, Katzerke C, et al. Disruption of the C/EBPalpha-miR-182 balance impairs granulocytic differentiation. Nat Commun. 2017;8:46. [PubMed: 28663557]

[64]. Muraleedharan CK, McClellan SA, Barrett RP, Li C, Montenegro D, Carion T, et al. Inactivation of the miR-183/96/182 Cluster Decreases the Severity of Pseudomonas aeruginosa-Induced Keratitis. Invest Ophthalmol Vis Sci. 2016;57:1506–17. [PubMed: 27035623]

[65]. Muraleedharan CK, McClellan SA, Ekanayaka SA, Francis R, Zmejkoski A, Hazlett LD, et al. The miR-183/96/182 Cluster Regulates Macrophage Functions in Response to Pseudomonas aeruginosa. J Innate Immun. 2019:1–12.

[66]. Wang J, Li G, Wu X, Liu Q, Yin C, Brown SL, et al. miR-183-96-182 Cluster Is Involved in Invariant NKT Cell Development, Maturation, and Effector Function. J Immunol. 2019.

[67]. Satija R, Farrell JA, Gennert D, Schier AF, Regev A. Spatial reconstruction of single-cell gene expression data. Nat Biotechnol. 2015;33:495–502. [PubMed: 25867923]

[68]. Aran D, Looney AP, Liu L, Wu E, Fong V, Hsu A, et al. Reference-based analysis of lung single-cell sequencing reveals a transitional profibrotic macrophage. Nat Immunol. 2019;20:163–72. [PubMed: 30643263]

[69]. Lewis BP, Burge CB, Bartel DP. Conserved seed pairing, often flanked by adenosines, indicates that thousands of human genes are microRNA targets. Cell. 2005;120:15–20. [PubMed: 15652477]

[70]. Grimson A, Farh KK, Johnston WK, Garrett-Engele P, Lim LP, Bartel DP. MicroRNA targeting specificity in mammals: determinants beyond seed pairing. Mol Cell. 2007;27:91–105. [PubMed: 17612493]

[71]. Huang da W, Sherman BT, Lempicki RA. Systematic and integrative analysis of large gene lists using DAVID bioinformatics resources. Nat Protoc. 2009;4:44–57. [PubMed: 19131956]

[72]. Eden E, Navon R, Steinfeld I, Lipson D, Yakhini Z. GOrilla: a tool for discovery and visualization of enriched GO terms in ranked gene lists. BMC Bioinformatics. 2009;10:48. [PubMed: 19192299]

[73]. Supek F, Bosnjak M, Skunca N, Smuc T. REVIGO summarizes and visualizes long lists of gene ontology terms. PLoS One. 2011;6:e21800. [PubMed: 21789182]

[74]. Lumayag S, Haldin CE, Corbett NJ, Wahlin KJ, Cowan C, Turturro S, et al. Inactivation of the microRNA-183/96/182 cluster results in syndromic retinal degeneration. Proceedings of the National Academy of Sciences of the United States of America. 2013;110:E507–E16. [PubMed: 23341629]

[75]. Liu CY, Zhu G, Westerhausen-Larson A, Converse R, Kao CW, Sun TT, et al. Cornea-specific expression of K12 keratin during mouse development. Curr Eye Res. 1993;12:963–74. [PubMed: 7508359]

[76]. Shaham O, Menuchin Y, Farhy C, Ashery-Padan R. Pax6: a multi-level regulator of ocular development. Prog Retin Eye Res. 2012;31:351–76. [PubMed: 22561546]

[77]. Rubsam M, Broussard JA, Wickstrom SA, Nekrasova O, Green KJ, Niessen CM. Adherens Junctions and Desmosomes Coordinate Mechanics and Signaling to Orchestrate Tissue Morphogenesis and Function: An Evolutionary Perspective. Cold Spring Harb Perspect Biol. 2018;10.

[78]. Sun TT, Eichner R, Nelson WG, Tseng SC, Weiss RA, Jarvinen M, et al. Keratin classes: molecular markers for different types of epithelial differentiation. J Invest Dermatol. 1983;81:109s–15s. [PubMed: 6190956]

[79]. Tsukita S, Tanaka H, Tamura A. The Claudins: From Tight Junctions to Biological Systems. Trends Biochem Sci. 2019;44:141–52. [PubMed: 30665499]

[80]. Gipson IK. Distribution of mucins at the ocular surface. Exp Eye Res. 2004;78:379–88. [PubMed: 15106916]

[81]. Schermer A, Jester JV, Hardy C, Milano D, Sun TT. Transient synthesis of K6 and K16 keratins in regenerating rabbit corneal epithelium: keratin markers for an alternative pathway of keratinocyte differentiation. Differentiation. 1989;42:103–10. [PubMed: 2483836]

[82]. Jaworski CJ, Aryankalayil-John M, Campos MM, Fariss RN, Rowsey J, Agarwalla N, et al. Expression analysis of human pterygium shows a predominance of conjunctival and limbal markers and genes associated with cell migration. Mol Vis. 2009;15:2421–34. [PubMed: 19956562]

[83]. Argueso P, Gipson IK. Epithelial mucins of the ocular surface: structure, biosynthesis and function. Exp Eye Res. 2001;73:281–9. [PubMed: 11520103]

[84]. Pflugfelder SC, Liu Z, Monroy D, Li DQ, Carvajal ME, Price-Schiavi SA, et al. Detection of sialomucin complex (MUC4) in human ocular surface epithelium and tear fluid. Invest Ophthalmol Vis Sci. 2000;41:1316–26. [PubMed: 10798646]

[85]. Carraway KL, Price-Schiavi SA, Komatsu M, Idris N, Perez A, Li P, et al. Multiple facets of sialomucin complex/MUC4, a membrane mucin and erbb2 ligand, in tumors and tissues (Y2K update). Front Biosci. 2000;5:D95–D107. [PubMed: 10702370]

[86]. Woodward AM, Argueso P. Expression analysis of the transmembrane mucin MUC20 in human corneal and conjunctival epithelia. Invest Ophthalmol Vis Sci. 2014;55:6132–8. [PubMed: 25168902]

[87]. Yoshida S, Shimmura S, Kawakita T, Miyashita H, Den S, Shimazaki J, et al. Cytokeratin 15 can be used to identify the limbal phenotype in normal and diseased ocular surfaces. Invest Ophthalmol Vis Sci. 2006;47:4780–6. [PubMed: 17065488]

[88]. Pan SH, Zhao N, Feng X, Jie Y, Jin ZB. Conversion of mouse embryonic fibroblasts into neural crest cells and functional corneal endothelia by defined small molecules. Sci Adv. 2021;7.

[89]. Verkman AS. Aquaporin water channels and endothelial cell function. J Anat. 2002;200:617–27. [PubMed: 12162729]

[90]. Bartakova A, Alvarez-Delfin K, Weisman AD, Salero E, Raffa GA, Merkhofer RM Jr., et al. Novel Identity and Functional Markers for Human Corneal Endothelial Cells. Invest Ophthalmol Vis Sci. 2016;57:2749–62. [PubMed: 27196322]

[91]. Okumura N, Hirano H, Numata R, Nakahara M, Ueno M, Hamuro J, et al. Cell surface markers of functional phenotypic corneal endothelial cells. Invest Ophthalmol Vis Sci. 2014;55:7610–8. [PubMed: 25389199]

[92]. Ginhoux F, Jung S. Monocytes and macrophages: developmental pathways and tissue homeostasis. Nat Rev Immunol. 2014;14:392–404. [PubMed: 24854589]

[93]. Hamrah P, Zhang Q, Liu Y, Dana MR. Novel characterization of MHC class II-negative population of resident corneal Langerhans cell-type dendritic cells. Invest Ophthalmol Vis Sci. 2002;43:639–46. [PubMed: 11867578]

[94]. Guilliams M, Ginhoux F, Jakubzick C, Naik SH, Onai N, Schraml BU, et al. Dendritic cells, monocytes and macrophages: a unified nomenclature based on ontogeny. Nat Rev Immunol. 2014;14:571–8. [PubMed: 25033907]

[95]. Mizumoto N, Takashima A. CD1a and langerin: acting as more than Langerhans cell markers. J Clin Invest. 2004;113:658–60. [PubMed: 14991060]

[96]. Mildner A, Jung S. Development and function of dendritic cell subsets. Immunity. 2014;40:642–56. [PubMed: 24837101]

[97]. Heng TS, Painter MW, Immunological Genome Project C. The Immunological Genome Project: networks of gene expression in immune cells. Nat Immunol. 2008;9:1091–4. [PubMed: 18800157]

[98]. Trapnell C, Cacchiarelli D, Grimsby J, Pokharel P, Li S, Morse M, et al. The dynamics and regulators of cell fate decisions are revealed by pseudotemporal ordering of single cells. Nat Biotechnol. 2014;32:381–6. [PubMed: 24658644]

[99]. Viola A, Munari F, Sanchez-Rodriguez R, Scolaro T, Castegna A. The Metabolic Signature of Macrophage Responses. Frontiers in immunology. 2019;10:1462. [PubMed: 31333642]

[100]. Ryan DG, O'Neill LAJ. Krebs Cycle Reborn in Macrophage Immunometabolism. Annu Rev Immunol. 2020;38:289–313. [PubMed: 31986069]

[101]. Stout RD, Suttles J. Functional plasticity of macrophages: reversible adaptation to changing microenvironments. J Leukoc Biol. 2004;76:509–13. [PubMed: 15218057]

[102]. Mitsi E, Kamng'ona R, Rylance J, Solorzano C, Jesus Reine J, Mwandumba HC, et al. Human alveolar macrophages predominately express combined classical M1 and M2 surface markers in steady state. Respir Res. 2018;19:66. [PubMed: 29669565]

[103]. Witherel CE, Sao K, Brisson BK, Han B, Volk SW, Petrie RJ, et al. Regulation of extracellular matrix assembly and structure by hybrid M1/M2 macrophages. Biomaterials. 2021;269:120667. [PubMed: 33450585]

[104]. Mor-Vaknin N, Punturieri A, Sitwala K, Markovitz DM. Vimentin is secreted by activated macrophages. Nat Cell Biol. 2003;5:59–63. [PubMed: 12483219]

[105]. Argueso P, Guzman-Aranguez A, Mantelli F, Cao Z, Ricciuto J, Panjwani N. Association of cell surface mucins with galectin-3 contributes to the ocular surface epithelial barrier. J Biol Chem. 2009;284:23037–45. [PubMed: 19556244]

[106]. Uchino Y, Mauris J, Woodward AM, Dieckow J, Amparo F, Dana R, et al. Alteration of galectin-3 in tears of patients with dry eye disease. Am J Ophthalmol. 2015;159:1027–35 e3. [PubMed: 25703476]

[107]. Han KE, Choi SI, Kim TI, Maeng YS, Stulting RD, Ji YW, et al. Pathogenesis and treatments of TGFBI corneal dystrophies. Prog Retin Eye Res. 2016;50:67–88. [PubMed: 26612778]

[108]. Dyrlund TF, Poulsen ET, Scavenius C, Nikolajsen CL, Thogersen IB, Vorum H, et al. Human cornea proteome: identification and quantitation of the proteins of the three main layers including epithelium, stroma, and endothelium. J Proteome Res. 2012;11:4231–9. [PubMed: 22698189]

[109]. Runager K, Klintworth GK, Karring H, Enghild JJ. The insoluble TGFBIp fraction of the cornea is covalently linked via a disulfide bond to type XII collagen. Biochemistry. 2013;52:2821–7. [PubMed: 23556985]

[110]. Billings PC, Whitbeck JC, Adams CS, Abrams WR, Cohen AJ, Engelsberg BN, et al. The transforming growth factor-beta-inducible matrix protein (beta)ig-h3 interacts with fibronectin. J Biol Chem. 2002;277:28003–9. [PubMed: 12034705]

[111]. Saika S, Sumioka T, Okada Y, Yamanaka O, Kitano A, Miyamoto T, et al. Wakayama symposium: modulation of wound healing response in the corneal stroma by osteopontin and tenascin-C. The ocular surface. 2013;11:12–5. [PubMed: 23321354]

[112]. Miyazaki K, Okada Y, Yamanaka O, Kitano A, Ikeda K, Kon S, et al. Corneal wound healing in an osteopontin-deficient mouse. Invest Ophthalmol Vis Sci. 2008;49:1367–75. [PubMed: 18385052]

[113]. Rittling SR. Osteopontin in macrophage function. Expert Rev Mol Med. 2011;13:e15. [PubMed: 21545755]

[114]. Filiberti A, Gmyrek GB, Montgomery ML, Sallack R, Carr DJJ. Loss of Osteopontin Expression Reduces HSV-1-Induced Corneal Opacity. Invest Ophthalmol Vis Sci. 2020;61:24.

[115]. Shinzawa M, Dogru M, Den S, Ichijima T, Higa K, Kojima T, et al. Epidermal Fatty Acid-Binding Protein: A Novel Marker in the Diagnosis of Dry Eye Disease in Sjogren Syndrome. Int J Mol Sci. 2018;19. [PubMed: 30577572]

[116]. Hotamisligil GS, Bernlohr DA. Metabolic functions of FABPs--mechanisms and therapeutic implications. Nat Rev Endocrinol. 2015;11:592–605. [PubMed: 26260145]

[117]. Chen S, Young MF, Chakravarti S, Birk DE. Interclass small leucine-rich repeat proteoglycan interactions regulate collagen fibrillogenesis and corneal stromal assembly. Matrix Biol. 2014;35:103–11. [PubMed: 24447998]

[118]. Zhang W, Ge Y, Cheng Q, Zhang Q, Fang L, Zheng J. Decorin is a pivotal effector in the extracellular matrix and tumour microenvironment. Oncotarget. 2018;9:5480–91. [PubMed: 29435195]

[119]. Larin SS, Gorlina NK, Kozlov IG, Cheredeev AN, Zorin NA, Zorina RM. Binding of alpha2-macroglobulin to collagen type I: modification of collagen matrix by alpha2-macroglobulin induces the enhancement of macrophage migration. Russ J Immunol. 2002;7:34–40. [PubMed: 12687264]

[120]. Bucala R, Spiegel LA, Chesney J, Hogan M, Cerami A. Circulating fibrocytes define a new leukocyte subpopulation that mediates tissue repair. Mol Med. 1994;1:71–81. [PubMed: 8790603]

[121]. Reilkoff RA, Bucala R, Herzog EL. Fibrocytes: emerging effector cells in chronic inflammation. Nat Rev Immunol. 2011;11:427–35. [PubMed: 21597472]

[122]. Bucala R. Fibrocytes at 20 Years. Mol Med. 2015;21 Suppl 1:S3–5. [PubMed: 26605645]

[123]. Reinhardt JW, Breuer CK. Fibrocytes: A Critical Review and Practical Guide. Frontiers in immunology. 2021;12:784401. [PubMed: 34975874]

[124]. Wilson SE. TGF beta −1, −2 and −3 in the modulation of fibrosis in the cornea and other organs. Exp Eye Res. 2021;207:108594. [PubMed: 33894227]

[125]. Tandon A, Tovey JC, Sharma A, Gupta R, Mohan RR. Role of transforming growth factor Beta in corneal function, biology and pathology. Curr Mol Med. 2010;10:565–78. [PubMed: 20642439]

[126]. Zhang F, Liu K, Zhao H, He Y. The emerging role of fibrocytes in ocular disorders. Stem Cell Res Ther. 2018;9:105. [PubMed: 29653588]

[127]. de Oliveira RC, Wilson SE. Fibrocytes, Wound Healing, and Corneal Fibrosis. Invest Ophthalmol Vis Sci. 2020;61:28.

[128]. Chesney J, Metz C, Stavitsky AB, Bacher M, Bucala R. Regulated production of type I collagen and inflammatory cytokines by peripheral blood fibrocytes. J Immunol. 1998;160:419–25. [PubMed: 9551999]

[129]. Gillespie M, Jassal B, Stephan R, Milacic M, Rothfels K, Senff-Ribeiro A, et al. The reactome pathway knowledgebase 2022. Nucleic Acids Res. 2022;50:D687–D92. [PubMed: 34788843]

[130]. Miller I, Min M, Yang C, Tian C, Gookin S, Carter D, et al. Ki67 is a Graded Rather than a Binary Marker of Proliferation versus Quiescence. Cell Rep. 2018;24:1105–12 e5. [PubMed: 30067968]

[131]. Gautier EL, Shay T, Miller J, Greter M, Jakubzick C, Ivanov S, et al. Gene-expression profiles and transcriptional regulatory pathways that underlie the identity and diversity of mouse tissue macrophages. Nat Immunol. 2012;13:1118–28. [PubMed: 23023392]

[132]. Simoni Y, Newell EW. Toward Meaningful Definitions of Innate-Lymphoid-Cell Subsets. Immunity. 2017;46:760–1. [PubMed: 28514678]

[133]. Spits H, Artis D, Colonna M, Diefenbach A, Di Santo JP, Eberl G, et al. Innate lymphoid cells--a proposal for uniform nomenclature. Nat Rev Immunol. 2013;13:145–9. [PubMed: 23348417]

[134]. Godfrey DI, MacDonald HR, Kronenberg M, Smyth MJ, Van Kaer L. Opinion - NKT cells: what's in a name? Nature Reviews Immunology. 2004;4:231–7.

[135]. Crosby CM, Kronenberg M. Tissue-specific functions of invariant natural killer T cells. Nat Rev Immunol. 2018;18:559–74. [PubMed: 29967365]

[136]. Nau D, Altmayer N, Mattner J. Mechanisms of Innate Lymphoid Cell and Natural Killer T Cell Activation during Mucosal Inflammation. Journal of Immunology Research. 2014;2014.

[137]. Castillo-Gonzalez R, Cibrian D, Sanchez-Madrid F. Dissecting the complexity of gammadelta T-cell subsets in skin homeostasis, inflammation, and malignancy. J Allergy Clin Immunol. 2021;147:2030–42. [PubMed: 33259837]

[138]. Nielsen MM, Witherden DA, Havran WL. gammadelta T cells in homeostasis and host defence of epithelial barrier tissues. Nat Rev Immunol. 2017;17:733–45. [PubMed: 28920588]

[139]. Muro R, Takayanagi H, Nitta T. T cell receptor signaling for gammadeltaT cell development. Inflamm Regen. 2019;39:6. [PubMed: 30976362]

[140]. Ribot JC, Lopes N, Silva-Santos B. gammadelta T cells in tissue physiology and surveillance. Nat Rev Immunol. 2021;21:221–32. [PubMed: 33057185]

[141]. Li J, Tan G, Ding X, Wang Y, Wu A, Yang Q, et al. A mouse dry eye model induced by topical administration of the air pollutant particulate matter 10. Biomed Pharmacother. 2017;96:524–34. [PubMed: 29032336]

[142]. Tan G, Li J, Yang Q, Wu A, Qu DY, Wang Y, et al. Air pollutant particulate matter 2.5 induces dry eye syndrome in mice. Scientific reports. 2018;8:17828. [PubMed: 30546125]

[143]. Ligocki AJ, Fury W, Gutierrez C, Adler C, Yang T, Ni M, et al. Molecular characteristics and spatial distribution of adult human corneal cell subtypes. Scientific reports. 2021;11:16323. [PubMed: 34381080]

[144]. Wang Q, Dou S, Zhang B, Jiang H, Qi X, Duan H, et al. Heterogeneity of human corneal endothelium implicates lncRNA NEAT1 in Fuchs endothelial corneal dystrophy. Mol Ther Nucleic Acids. 2022;27:880–93. [PubMed: 35141048]

[145]. van Zyl T, Yan W, McAdams AM, Monavarfeshani A, Hageman GS, Sanes JR. Cell atlas of the human ocular anterior segment: Tissue-specific and shared cell types. Proc Natl Acad Sci U S A. 2022;119:e2200914119. [PubMed: 35858321]

[146]. Phillipson M, Kubes P. The neutrophil in vascular inflammation. Nat Med. 2011;17:1381–90. [PubMed: 22064428]

[147]. Kubes P. The enigmatic neutrophil: what we do not know. Cell Tissue Res. 2018;371:399–406. [PubMed: 29404726]

[148]. De Filippo K, Rankin SM. The Secretive Life of Neutrophils Revealed by Intravital Microscopy. Front Cell Dev Biol. 2020;8:603230. [PubMed: 33240898]

[149]. Casanova-Acebes M, Nicolas-Avila JA, Li JL, Garcia-Silva S, Balachander A, Rubio-Ponce A, et al. Neutrophils instruct homeostatic and pathological states in naive tissues. J Exp Med. 2018;215:2778–95. [PubMed: 30282719]

[150]. Puga I, Cols M, Barra CM, He B, Cassis L, Gentile M, et al. B cell-helper neutrophils stimulate the diversification and production of immunoglobulin in the marginal zone of the spleen. Nat Immunol. 2011;13:170–80. [PubMed: 22197976]

[151]. Deniset JF, Surewaard BG, Lee WY, Kubes P. Splenic Ly6G(high) mature and Ly6G(int) immature neutrophils contribute to eradication of S. pneumoniae. J Exp Med. 2017;214:1333–50. [PubMed: 28424248]

[152]. Bogoslowski A, Butcher EC, Kubes P. Neutrophils recruited through high endothelial venules of the lymph nodes via PNAd intercept disseminating Staphylococcus aureus. Proc Natl Acad Sci U S A. 2018;115:2449–54. [PubMed: 29378967]

[153]. Becher B, Schlitzer A, Chen J, Mair F, Sumatoh HR, Teng KW, et al. High-dimensional analysis of the murine myeloid cell system. Nat Immunol. 2014;15:1181–9. [PubMed: 25306126]

[154]. Ballesteros I, Rubio-Ponce A, Genua M, Lusito E, Kwok I, Fernandez-Calvo G, et al. Co-option of Neutrophil Fates by Tissue Environments. Cell. 2020;183:1282–97 e18. [PubMed: 33098771]

[155]. Hazlett LD, Zucker M, Berk RS. Distribution and kinetics of the inflammatory cell response to ocular challenge with Pseudomonas aeruginosa in susceptible versus resistant mice. Ophthalmic Res. 1992;24:32–9.

[156]. Kernacki KA, Barrett RP, Hobden JA, Hazlett LD. Macrophage inflammatory protein-2 is a mediator of polymorphonuclear neutrophil influx in ocular bacterial infection. J Immunol. 2000;164:1037–45. [PubMed: 10623854]

[157]. Metz CN. Fibrocytes: a unique cell population implicated in wound healing. Cell Mol Life Sci. 2003;60:1342–50. [PubMed: 12943223]

[158]. Blakaj A, Bucala R. Fibrocytes in health and disease. Fibrogenesis Tissue Repair. 2012;5:S6. [PubMed: 23259722]

[159]. Grieb G, Steffens G, Pallua N, Bernhagen J, Bucala R. Circulating fibrocytes--biology and mechanisms in wound healing and scar formation. Int Rev Cell Mol Biol. 2011;291:1–19. [PubMed: 22017972]

[160]. Grieb G, Bucala R. Fibrocytes in Fibrotic Diseases and Wound Healing. Adv Wound Care (New Rochelle). 2012;1:36–40. [PubMed: 24527276]

[161]. Lassance L, Marino GK, Medeiros CS, Thangavadivel S, Wilson SE. Fibrocyte migration, differentiation and apoptosis during the corneal wound healing response to injury. Exp Eye Res. 2018;170:177–87. [PubMed: 29481786]

[162]. De Roo AK, Wouters J, Govaere O, Foets B, van den Oord JJ. Identification of Circulating Fibrocytes and Dendritic Derivatives in Corneal Endothelium of Patients With Fuchs' Dystrophy. Invest Ophthalmol Vis Sci. 2017;58:670–81. [PubMed: 28135362]

[163]. Das SK, Gupta I, Cho YK, Zhang X, Uehara H, Muddana SK, et al. Vimentin knockdown decreases corneal opacity. Invest Ophthalmol Vis Sci. 2014;55:4030–40. [PubMed: 24854859]

[164]. SundarRaj N, Rizzo JD, Anderson SC, Gesiotto JP. Expression of vimentin by rabbit corneal epithelial cells during wound repair. Cell Tissue Res. 1992;267:347–56. [PubMed: 1376216]

[165]. Zhao G, Hu M, Li C, Lee J, Yuan K, Zhu G, et al. Osteopontin contributes to effective neutrophil recruitment, IL-1beta production and apoptosis in Aspergillus fumigatus keratitis. Immunol Cell Biol. 2018;96:401–12. [PubMed: 29359350]

[166]. Ablamowicz AF, Nichols JJ. Ocular Surface Membrane-Associated Mucins. The ocular surface. 2016;14:331–41. [PubMed: 27154035]

[167]. AbuSamra DB, Mauris J, Argueso P. Galectin-3 initiates epithelial-stromal paracrine signaling to shape the proteolytic microenvironment during corneal repair. Sci Signal. 2019;12.

[168]. Cao Z, Said N, Amin S, Wu HK, Bruce A, Garate M, et al. Galectins-3 and −7, but not galectin-1, play a role in re-epithelialization of wounds. J Biol Chem. 2002;277:42299–305. [PubMed: 12194966]

[169]. Eberl G, Colonna M, Di Santo JP, McKenzie AN. Innate lymphoid cells. Innate lymphoid cells: a new paradigm in immunology. Science. 2015;348:aaa6566. [PubMed: 25999512]

[170]. Artis D, Spits H. The biology of innate lymphoid cells. Nature. 2015;517:293–301. [PubMed: 25592534]

[171]. Panda SK, Colonna M. Innate Lymphoid Cells in Mucosal Immunity. Frontiers in immunology. 2019;10:861. [PubMed: 31134050]

[172]. Berzins SP, Ritchie DS. Natural killer T cells: drivers or passengers in preventing human disease? Nature Reviews Immunology. 2014;14:640–6.

[173]. Liu J, Xiao C, Wang H, Xue Y, Dong D, Lin C, et al. Local Group 2 Innate Lymphoid Cells Promote Corneal Regeneration after Epithelial Abrasion. Am J Pathol. 2017;187:1313–26. [PubMed: 28419818]

[174]. Hirose S, Wang S, Tormanen K, Wang Y, Tang J, Akbari O, et al. Roles of Type 1, 2, and 3 Innate Lymphoid Cells in Herpes Simplex Virus 1 Infection In Vitro and In Vivo. J Virol. 2019;93.

[175]. Chen Y, Chauhan SK, Saban DR, Sadrai Z, Okanobo A, Dana R. Interferon-gamma-secreting NK cells promote induction of dry eye disease. J Leukoc Biol. 2011;89:965–72. [PubMed: 21402771]

[176]. Liu Q, Smith CW, Zhang W, Burns AR, Li Z. NK cells modulate the inflammatory response to corneal epithelial abrasion and thereby support wound healing. Am J Pathol. 2012;181:452–62. [PubMed: 22728064]

[177]. Zhang X, Volpe EA, Gandhi NB, Schaumburg CS, Siemasko KF, Pangelinan SB, et al. NK cells promote Th-17 mediated corneal barrier disruption in dry eye. PLoS One. 2012;7:e36822. [PubMed: 22590618]

[178]. Lee H, Schlereth SL, Park EY, Emami-Naeini P, Chauhan SK, Dana R. A novel pro-angiogenic function for interferon-gamma-secreting natural killer cells. Invest Ophthalmol Vis Sci. 2014;55:2885–92. [PubMed: 24713481]

[179]. Hazlett LD, Li Q, Liu J, McClellan S, Du W, Barrett RP. NKT cells are critical to initiate an inflammatory response after Pseudomonas aeruginosa ocular infection in susceptible mice. J Immunol. 2007;179:1138–46. [PubMed: 17617607]

[180]. Sirajuddin N, Yin XT, Stuart PM. Role of NK T cells in transplantation with particular emphasis on corneal transplantation. Transpl Immunol. 2022;75:101727. [PubMed: 36183944]

[181]. Sonoda KH, Taniguchi M, Stein-Streilein J. Long-term survival of corneal allografts is dependent on intact CD1d-reactive NKT cells. J Immunol. 2002;168:2028–34. [PubMed: 11823540]

[182]. Sonoda KH, Stein-Streilein J. Ocular immune privilege and CD1d-reactive natural killer T cells. Cornea. 2002;21:S33–8. [PubMed: 11995808]

[183]. Jie Y, Pan Z, Xu L, Chen Y, Zhang W, Wu Y, et al. Upregulation of CD4+ NKT cells is important for allograft survival in staphylococcal-enterotoxin-B-treated rats after high-risk corneal transplantation. Ophthalmic Res. 2007;39:130–8. [PubMed: 17505144]

[184]. Oshima T, Sonoda KH, Nakao S, Hijioka K, Taniguchi M, Ishibashi T. Protective role for CD1d-reactive invariant natural killer T cells in cauterization-induced corneal inflammation. Invest Ophthalmol Vis Sci. 2008;49:105–12. [PubMed: 18172081]

[185]. Fitzpatrick S, Lausch R, Barrington RA. CCR6-Positive gammadelta T Cells Provide Protection Against Intracorneal HSV-1 Infection. Invest Ophthalmol Vis Sci. 2019;60:3952–62. [PubMed: 31560369]

[186]. He S, Zhang H, Liu S, Liu H, Chen G, Xie Y, et al. gammadelta T cells regulate the expression of cytokines but not the manifestation of fungal keratitis. Exp Eye Res. 2015;135:93–101. [PubMed: 25864785]

[187]. O'Brien RL, Taylor MA, Hartley J, Nuhsbaum T, Dugan S, Lahmers K, et al. Protective role of gammadelta T cells in spontaneous ocular inflammation. Invest Ophthalmol Vis Sci. 2009;50:3266–74. [PubMed: 19151391]

[188]. St Leger AJ, Desai JV, Drummond RA, Kugadas A, Almaghrabi F, Silver P, et al. An Ocular Commensal Protects against Corneal Infection by Driving an Interleukin-17 Response from Mucosal gammadelta T Cells. Immunity. 2017.

[189]. Nabi R, Lewin AC, Collantes TM, Chouljenko VN, Kousoulas KG. Intramuscular Vaccination With the HSV-1(VC2) Live-Attenuated Vaccine Strain Confers Protection Against Viral Ocular Immunopathogenesis Associated With gammadeltaT Cell Intracorneal Infiltration. Frontiers in immunology. 2021;12:789454. [PubMed: 34868077]

[190]. He J, Jiao X, Sun X, Huang Y, Xu P, Xue Y, et al. Short-Term High Fructose Intake Impairs Diurnal Oscillations in the Murine Cornea. Invest Ophthalmol Vis Sci. 2021;62:22.

[191]. Xiao C, Wu M, Liu J, Gu J, Jiao X, Lu D, et al. Acute tobacco smoke exposure exacerbates the inflammatory response to corneal wounds in mice via the sympathetic nervous system. Commun Biol. 2019;2:33. [PubMed: 30701198]

[192]. Reyes NJ, Mayhew E, Chen PW, Niederkorn JY. gammadelta T cells are required for maximal expression of allergic conjunctivitis. Invest Ophthalmol Vis Sci. 2011;52:2211–6. [PubMed: 21212171]

[193]. Cua DJ, Tato CM. Innate IL-17-producing cells: the sentinels of the immune system. Nat Rev Immunol. 2010;10:479–89. [PubMed: 20559326]

[194]. Hirota K, Duarte JH, Veldhoen M, Hornsby E, Li Y, Cua DJ, et al. Fate mapping of IL-17-producing T cells in inflammatory responses. Nat Immunol. 2011;12:255–63. [PubMed: 21278737]

[195]. Hirota K, Ahlfors H, Duarte JH, Stockinger B. Regulation and function of innate and adaptive interleukin-17-producing cells. EMBO Rep. 2012;13:113–20. [PubMed: 22193778]

[196]. Li J, Casanova JL, Puel A. Mucocutaneous IL-17 immunity in mice and humans: host defense vs. excessive inflammation. Mucosal Immunol. 2018;11:581–9. [PubMed: 29186107]

[197]. Mills KHG. IL-17 and IL-17-producing cells in protection versus pathology. Nat Rev Immunol. 2022:1–17. [PubMed: 34799725]

[198]. Bonnardel J, T'Jonck W, Gaublomme D, Browaeys R, Scott CL, Martens L, et al. Stellate Cells, Hepatocytes, and Endothelial Cells Imprint the Kupffer Cell Identity on Monocytes Colonizing the Liver Macrophage Niche. Immunity. 2019;51:638–54 e9. [PubMed: 31561945]

[199]. Weiss JS, Moller HU, Lisch W, Kinoshita S, Aldave AJ, Belin MW, et al. The IC3D classification of the corneal dystrophies. Cornea. 2008;27 Suppl 2:S1–83. [PubMed: 19337156]

[200]. Kotulak JC, Brungardt T. Age-related changes in the cornea. J Am Optom Assoc. 1980;51:761–5. [PubMed: 6969271]

[201]. Moshirfar M, Bennett P, Ronquillo Y. Corneal Dystrophy. StatPearls. Treasure Island (FL) 2022.

[202]. Ivaska J, Pallari HM, Nevo J, Eriksson JE. Novel functions of vimentin in cell adhesion, migration, and signaling. Exp Cell Res. 2007;313:2050–62. [PubMed: 17512929]

[203]. Danielsson F, Peterson MK, Caldeira Araujo H, Lautenschlager F, Gad AKB. Vimentin Diversity in Health and Disease. Cells. 2018;7.

[204]. Gupta SK, Masinick S, Garrett M, Hazlett LD. Pseudomonas aeruginosa lipopolysaccharide binds galectin-3 and other human corneal epithelial proteins. Infection and immunity. 1997;65:2747–53. [PubMed: 9199445]

[205]. Xiao Y, Yang J, Fu Z, Xiong Z, Zhang C, He D, et al. Inhibition of Galectin-3 Impairs Antifungal Immune Response in Fungal Keratitis. Dis Markers. 2022;2022:8316004. [PubMed: 35437453]

[206]. Gerdes J, Schwab U, Lemke H, Stein H. Production of a mouse monoclonal antibody reactive with a human nuclear antigen associated with cell proliferation. Int J Cancer. 1983;31:13–20. [PubMed: 6339421]

[207]. Oka S, Uramoto H, Shimokawa H, Iwanami T, Tanaka F. The expression of Ki-67, but not proliferating cell nuclear antigen, predicts poor disease free survival in patients with adenocarcinoma of the lung. Anticancer Res. 2011;31:4277–82. [PubMed: 22199292]

[208]. Sun X, Kaufman PD. Ki-67: more than a proliferation marker. Chromosoma. 2018;127:175–86. [PubMed: 29322240]

[209]. O'Koren EG, Mathew R, Saban DR. Fate mapping reveals that microglia and recruited monocyte-derived macrophages are definitively distinguishable by phenotype in the retina. Scientific reports. 2016;6:20636. [PubMed: 26856416]

[210]. Zikherman J, Doan K, Parameswaran R, Raschke W, Weiss A. Quantitative differences in CD45 expression unmask functions for CD45 in B-cell development, tolerance, and survival. Proc Natl Acad Sci U S A. 2012;109:E3–12. [PubMed: 22135465]

[211]. Rizzo D, Lotay A, Gachard N, Marfak I, Faucher JL, Trimoreau F, et al. Very low levels of surface CD45 reflect CLL cell fragility, are inversely correlated with trisomy 12 and are associated with increased treatment-free survival. Am J Hematol. 2013;88:747–53. [PubMed: 23733486]

[212]. Petkov S, Bekele Y, Lakshmikanth T, Hejdeman B, Zazzi M, Brodin P, et al. High CD45 expression of CD8+ and CD4+ T cells correlates with the size of HIV-1 reservoir in blood. Scientific reports. 2020;10:20425. [PubMed: 33235273]

[213]. Ahmed MGT, Limmer A, Sucker C, Fares KM, Mohamed SA, Othman AH, et al. Differential Regulation of CD45 Expression on Granulocytes, Lymphocytes, and Monocytes in COVID-19. J Clin Med. 2022;11.

## Highlights

- Corneal cellular composition and transcriptomes shift in naïve WT mice from 2 to 6 months old (mo), suggesting age-related adaptation to maintain homeostasis. Inactivation of miR-183C disrupted the stability of major cellular composition and age-related transcriptomic shifts of subtypes of corneal cells.
- The diversity of CRICs enhances with age. There exist previously unrecognized resident neutrophils and fibrocytes in naïve mouse cornea.
- Corneal resident macrophages (ResMϕ) adopt cornea-specific function by expressing extracellular matrix (ECM) and ECM organization-related genes.
- Adult naive cornea is endowed with partially differentiated, proliferative ResMϕ, providing a potential mechanism of quick amplification of functional Mϕ.
- The resident lymphocytes are comprised mainly of innate lymphoid cells (ILCs), followed by NKT and γδT cells. They are the major source of innate IL-17a.
- miR-183C limits the number and polarity development of ResMϕ, suggesting that miR-183C serves as a checkpoint for the differentiation of CRICs.

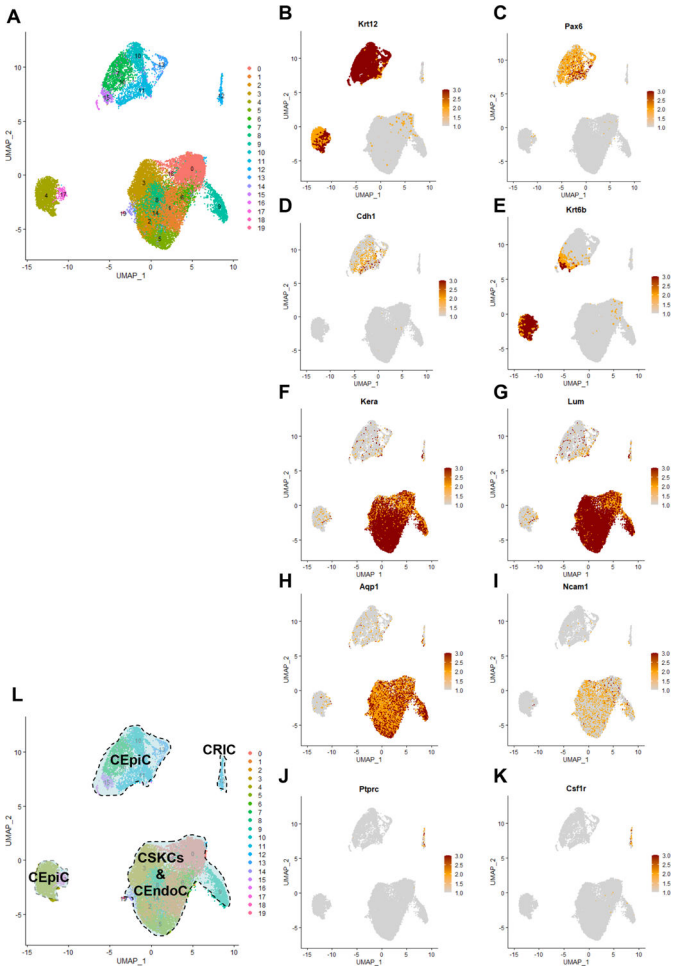


**Figure 1.**

Unbiased clustering of sc transcriptomes of total corneal cells. **A**. UMAP illustrating the distribution of 20 different clusters of total corneal cells. **B-K**. Distribution and levels of expression of corneal epithelial cell (CEpiC)(B-E), corneal stromal keratocyte (CSK) (F&G), corneal endothelial cell (CEndoC) (H&I), and corneal resident lymphocyte (CRL) markers (J&K). **L**. Collective distribution of annotated major corneal cell types in the UMAP.

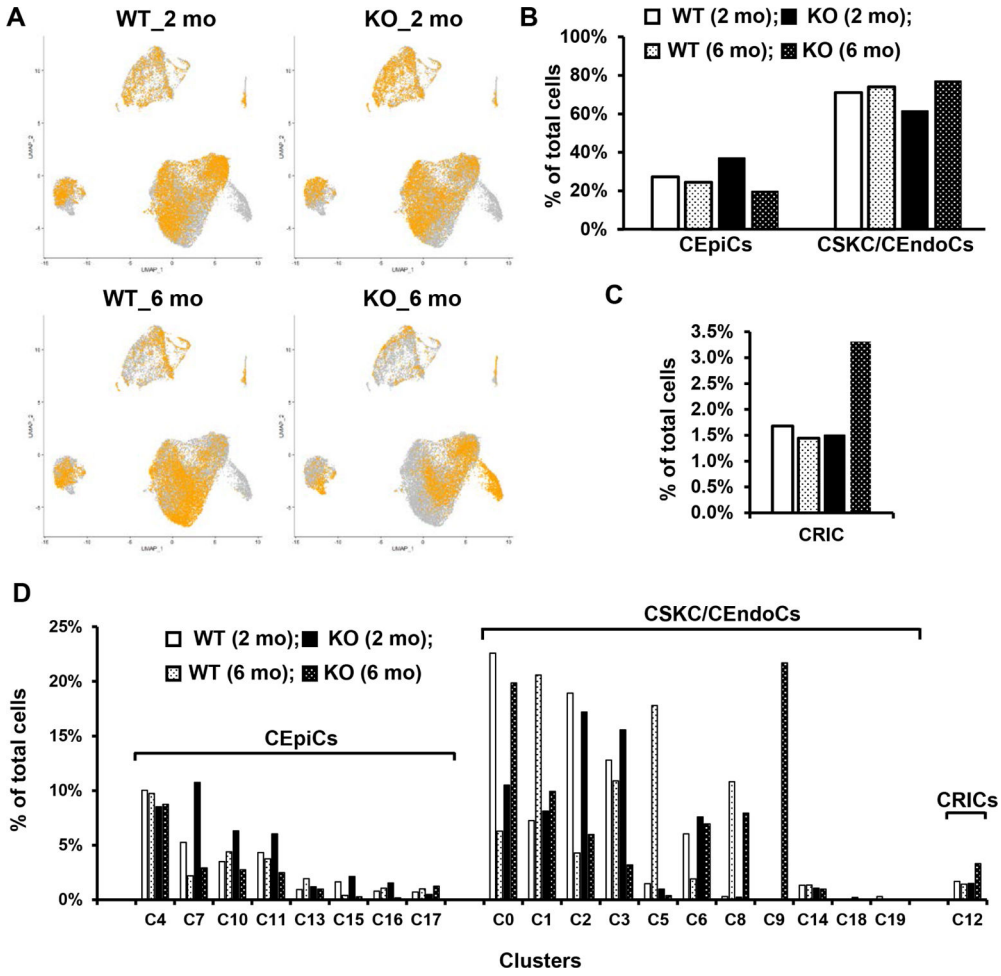


**Figure 2.**

miR-183C modulates the transcriptomic landscape of corneal cells. **A**. Distribution of total corneal cells from 2 and 6 mo WT and KO mice superimposed on the UMAP. **B & C**. Overall representation of major cell types, including CEpiCs, CSK/EndoCs (B) and CRICs (C) in total corneal cell samples of 2 and 6 mo WT and KO mice. D. Relative representation of all clusters in total corneal cell samples of 2 and 6 mo WT and KO mice.

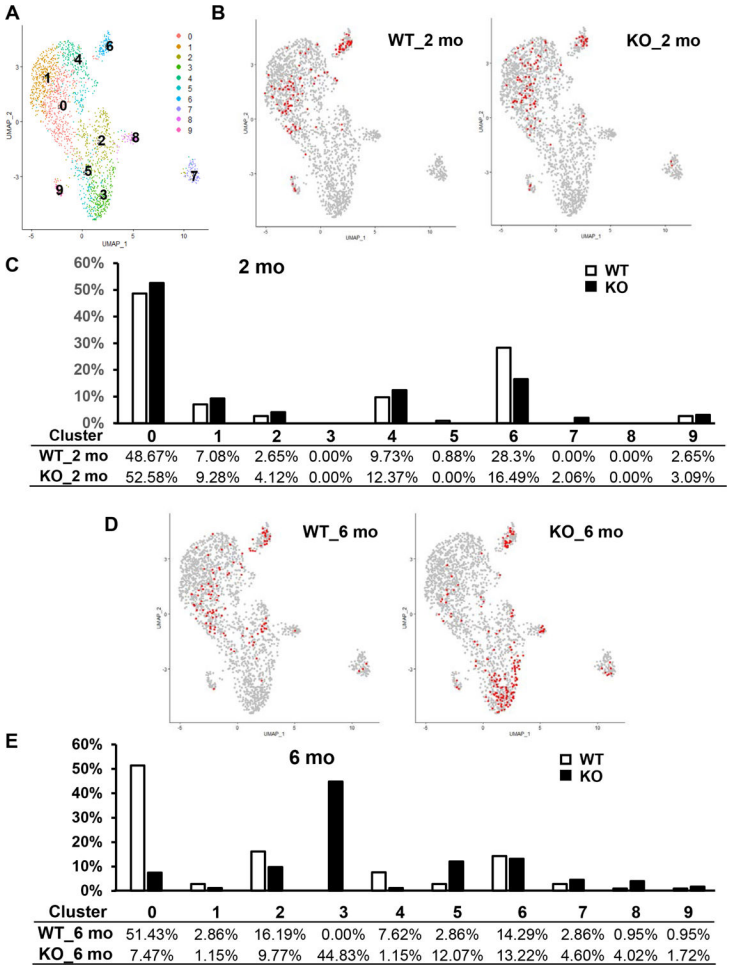


**Figure 3.**

miR-183C modulates the transcriptomic landscape of CRICs. **A**. UMAP illustrating the distribution of 10 clusters of the pooled CRICs; **B-E**. Inactivation of miR-183C results in changes of the relative representations of different clusters of CRICs in 2 mo (B&C) and 6 mo mice (D&E). B&D. Distribution of CRICs from the total corneal samples of 2 mo (B) and 6 mo (D) WT or KO mice superimposed on the UMAP of the pooled CRICs. C&E: Relative representation of different clusters of CRICs of 2 mo (C) and 6 mo (E) mice (based on data from total corneal cell samples).

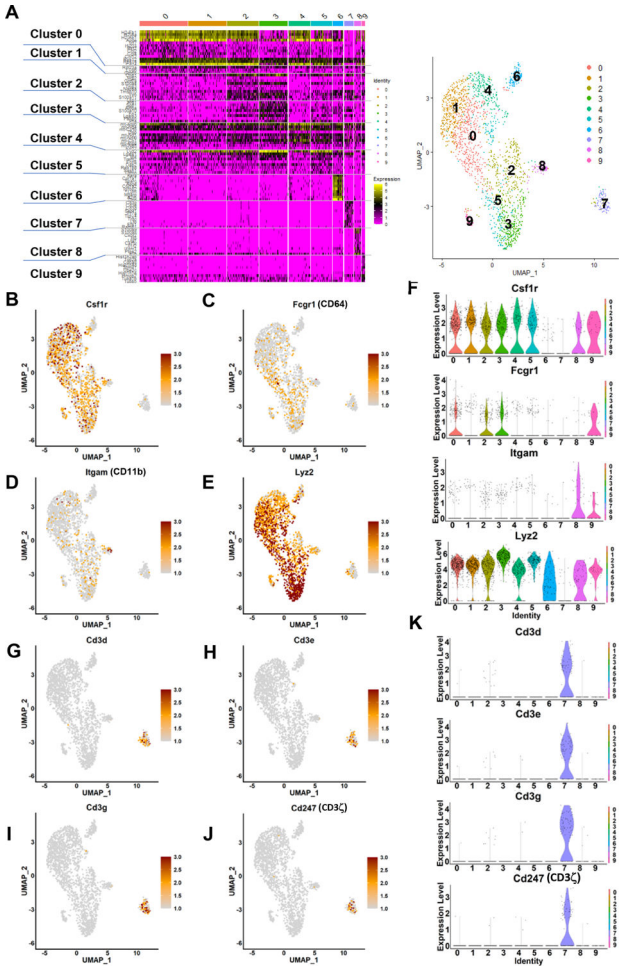


**Figure 4.**

Signature gene analysis of the pooled CRICs. **A**. Heatmap of signature genes of the 10 clusters of pooled CRICs; **B-K**. Distribution and levels of expression of myeloid (B-F) and lymphocyte marker (G-K) on the UMAP (B-E; G-J) or violin plots (F, K).

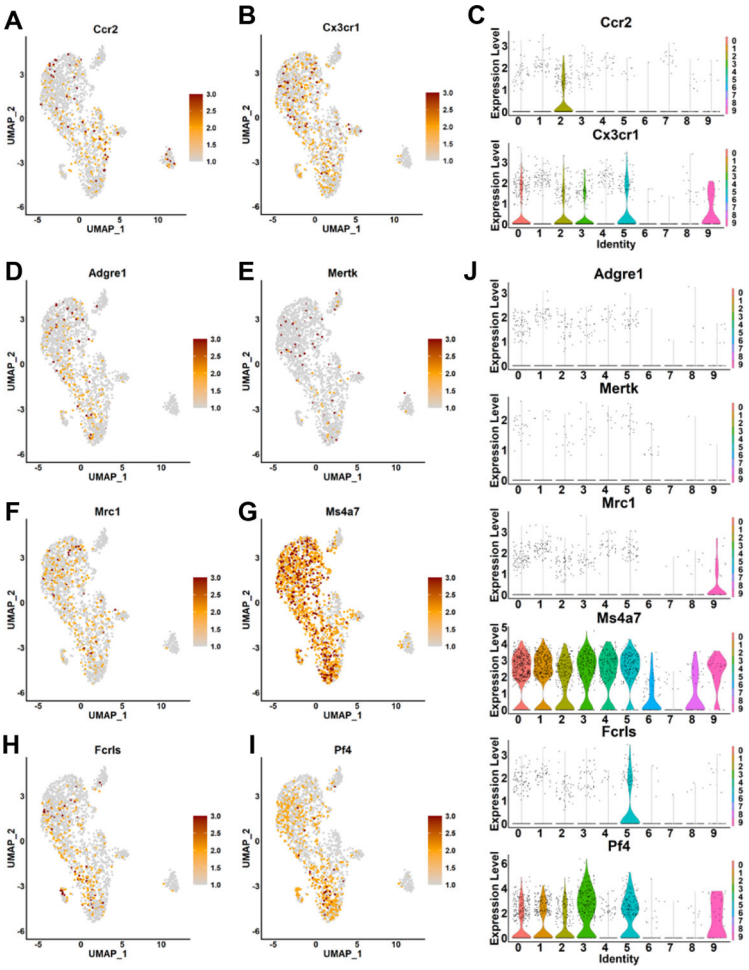


**Figure 5.**

Distribution and levels of expression of known monocyte (MC) (**A-C**) and macrophage (Mϕ)-marker genes in the pooled CRICs (**D-J**).

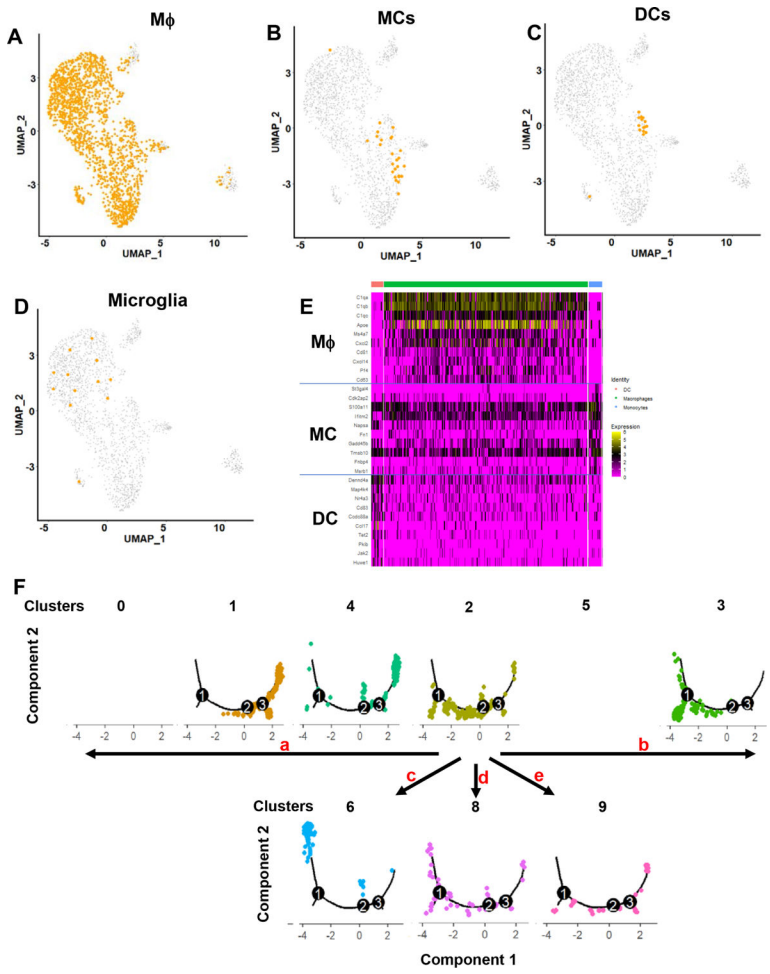


**Figure 6.**

Distribution of corneal resident Mϕ (**A**), MC (**B**), dendritic cells (DC) (**C**) and microglia (MG) (**D**) identified by SingleR/ImmGenData in the pooled CRICs. **E**. Heatmap of signature genes distinguishing Mϕ, MCs and DCs in Cluster 2. **F**. Distribution of different myeloid cell clusters in a single-cell trajectory map and hypothetical divergent directions of differentiation from Cluster 2 towards other myeloid clusters.

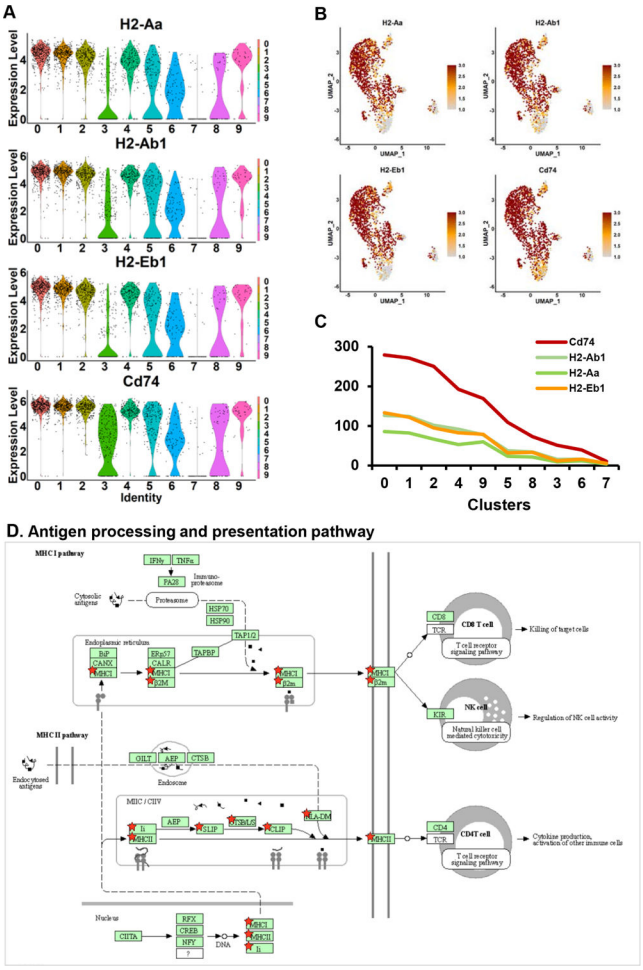


**Figure 7.**

Corneal ResMϕ are endowed with antigen processing and presentation (APP) markers. **A**. Violin plots; **B**. UMAP; **C**. Curve chart showing the expression of MHCII makers, H2Aa, H2Ab1 and H2-Eb1, and Cd74 in different clusters of the pooled CRICs. **D**. Signature genes of Cluster 0 are enriched in APP KEGG pathway. Star highlighted molecules or complexes are the ones in the signature genes of Cluster 0.

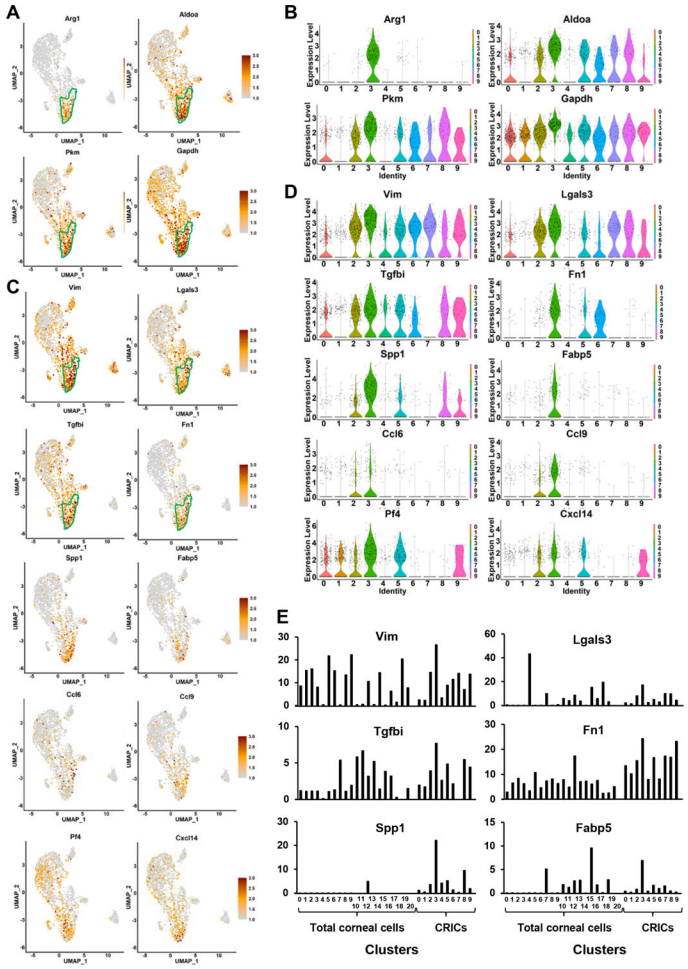


**Figure 8.**

Inactivation of miR-183C promotes M2 polarity and cornea-specific function of ECM production/organization in corneal ResMϕ. **A,C**. UMAP and **B, D**. Violin plots showing the distribution and expression levels of key genes involved in M2 polarity (Arg1), glycolysis (including Aldoa, Pkm, Gapdh), and genes involved in ECM production, organization and ECM-cell interactions. **E**. Comparison of average expression levels of ECM-related genes in different clusters of the pooled CRICs with the ones in the total corneal cells.

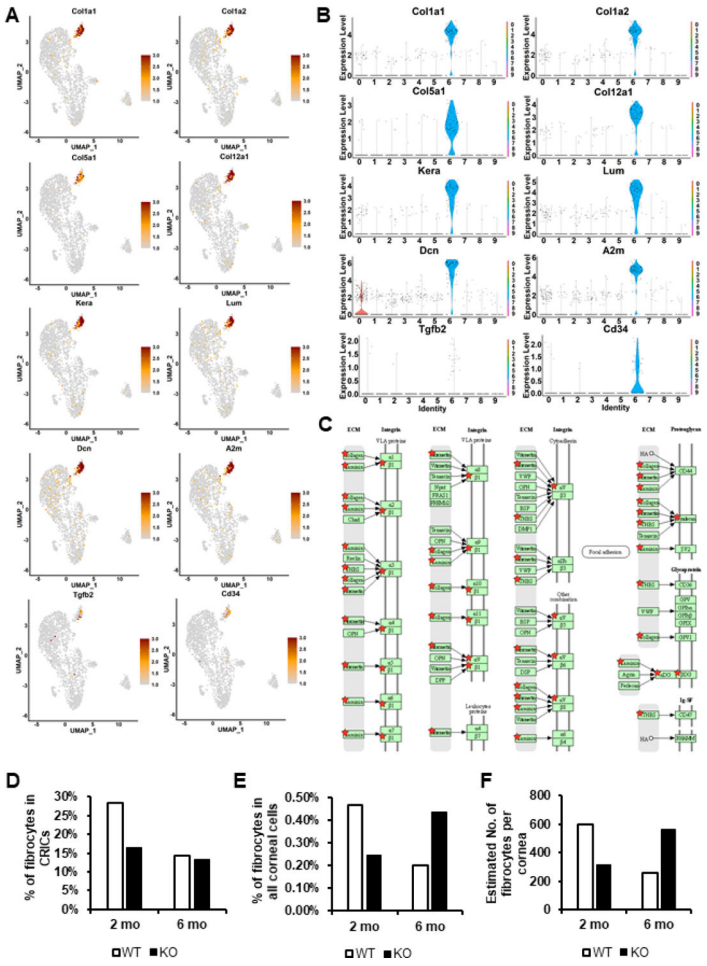


**Figure 9.**

The cornea is endowed with fibrocytes in Cluster 6. **A, B**: Expression patterns of signature genes of Cluster 6 which are involved in corneal ECM biogenesis and remodeling pathways, e.g. Col1a1, Col1a1, Col5a1, Col12a1, Kera and Lum, Dcn, A2m, Tgfb2, and hematopoietic cell marker, Cd34. **C**. Signatures genes of Cluster 6 are enriched in ECM-receptor interaction signaling pathway (KEGG). Star labeled are in signature genes of Cluster 6. The Cluster 6 signature genes involved in this pathway is listed in Table S22&S23. **D, E**. Percentage of fibrocytes in CRICs (D) or all corneal cells (E) categorized by age and genotypes. **F**. Estimated number of fibrocytes per cornea categorized by age and genotypes.

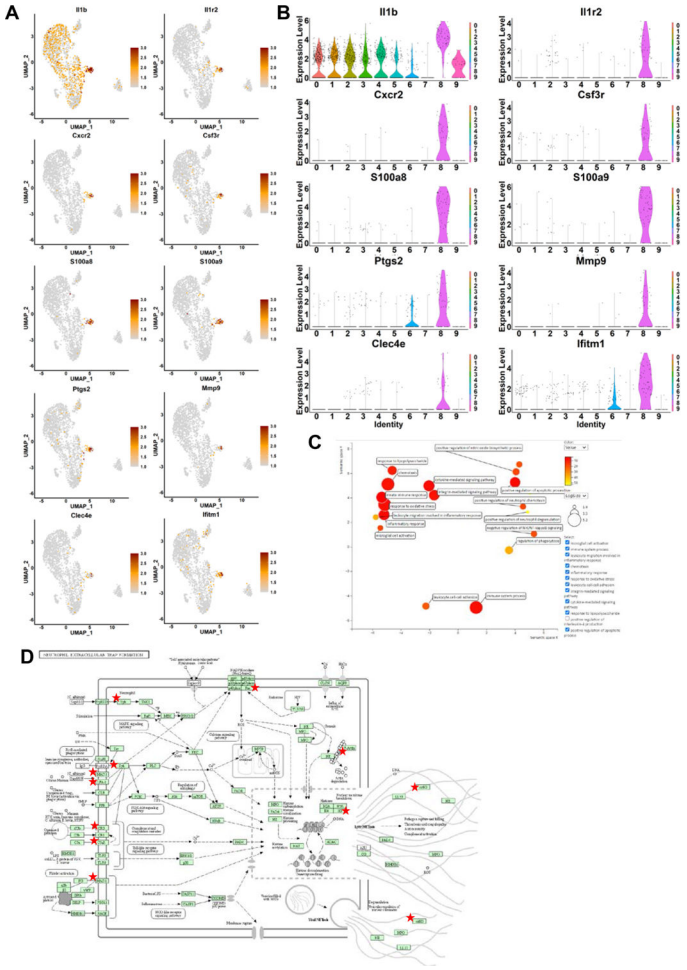


**Figure 10.**

Analyses of signature genes of Cluster 8 CRICs. **A&B**. Distribution and expression levels of Cluster 8 signature genes; **C**. GO analysis of the signature genes of Cluster 8 CRICs; **D**. Cluster 8 signature genes are enriched in the neutrophil extracellular trap formation signaling pathway (KEGG). Star labeled are in signature genes of Cluster 8.

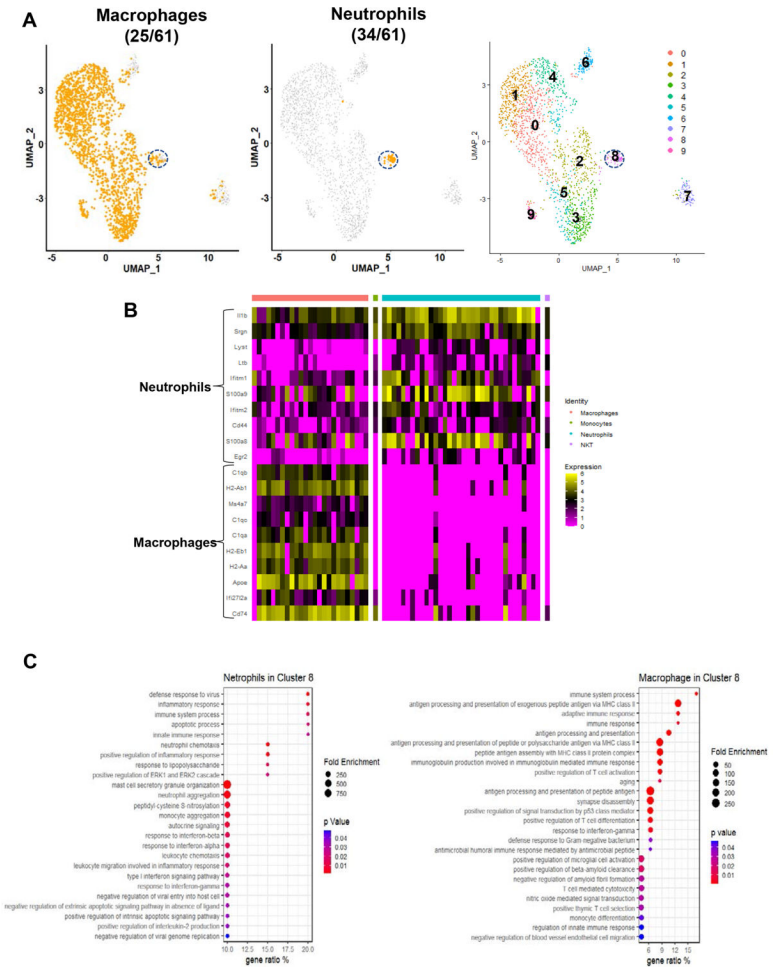


**Figure 11.**

**A**. Distribution of SingleR-identified Mϕ and neutrophils on the UMAP of the pooled CRICs. Cluster 8 is enriched neutrophils. **B**. Heatmap of top 10 signature genes of neutrophils and Mϕ of Cluster 8. **C**. GO analyses of signature genes of the neutrophils and Mϕ of Cluster 8

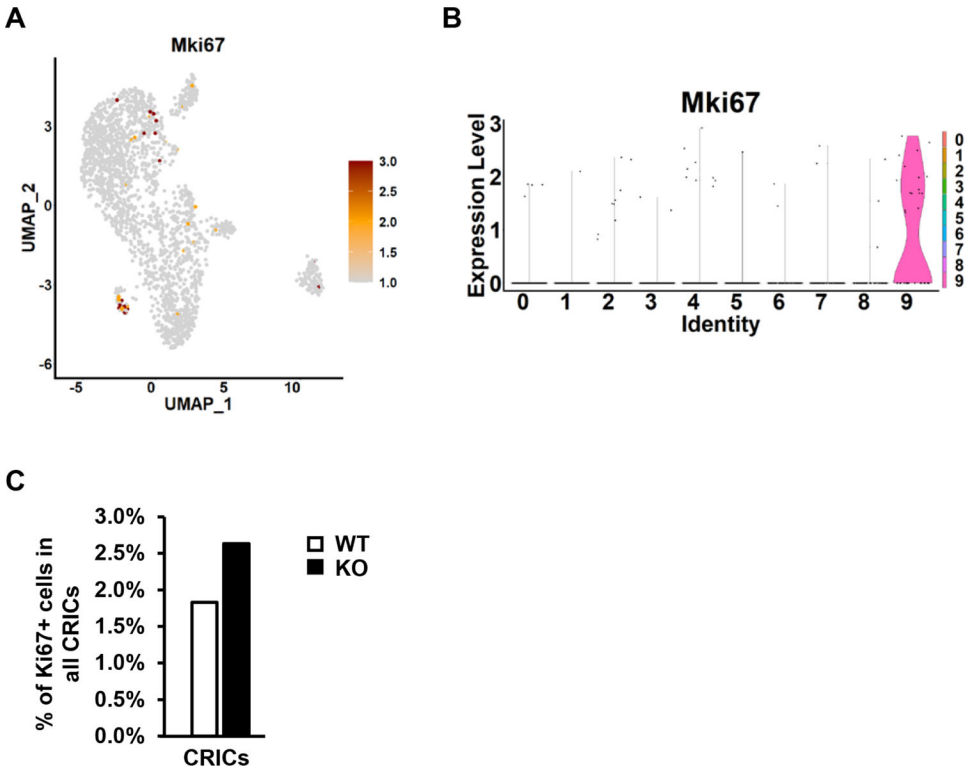


**Figure 12.**

Cluster 9 is enriched with proliferative cells. **A, B**. Distribution and expression levels of proliferative cell marker, Ki67; **C**. Relative representation of Ki67+ cells in all CRICs categorized by genotypes.

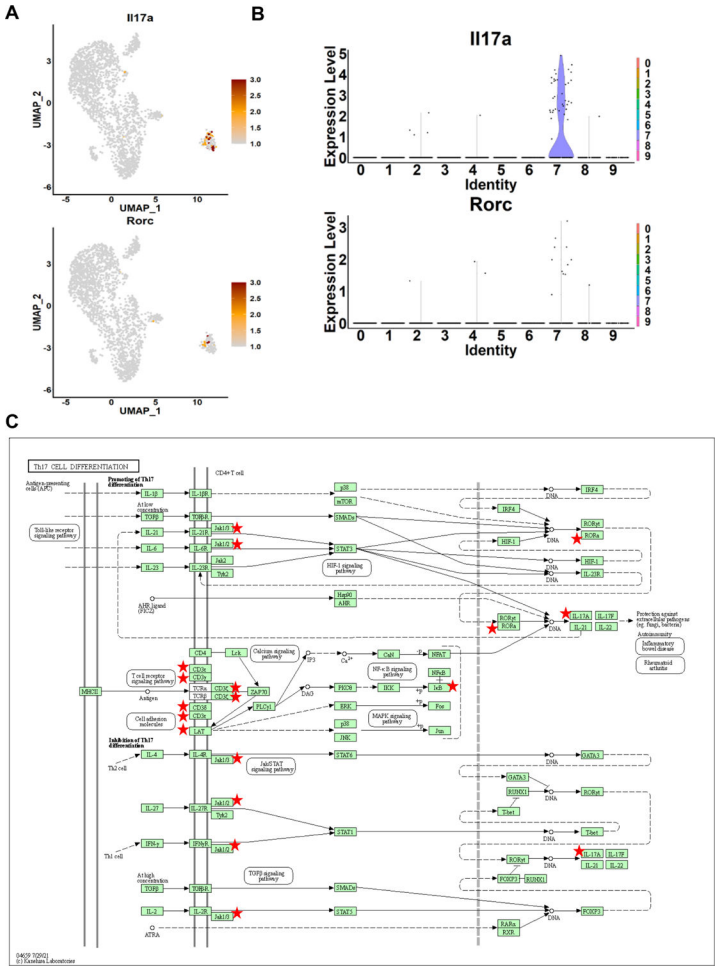


**Figure 13.**

miR-183C regulates corneal resident innate IL-17 producing lymphocytes. **A,B**. The distribution and levels of expression of IL-17a and Rorc in CRICs. **C**. Signature genes of Cluster 7 are enriched in Th17 cell differentiation signaling pathway. Star labeled molecules are in the signature genes of Cluster 7.

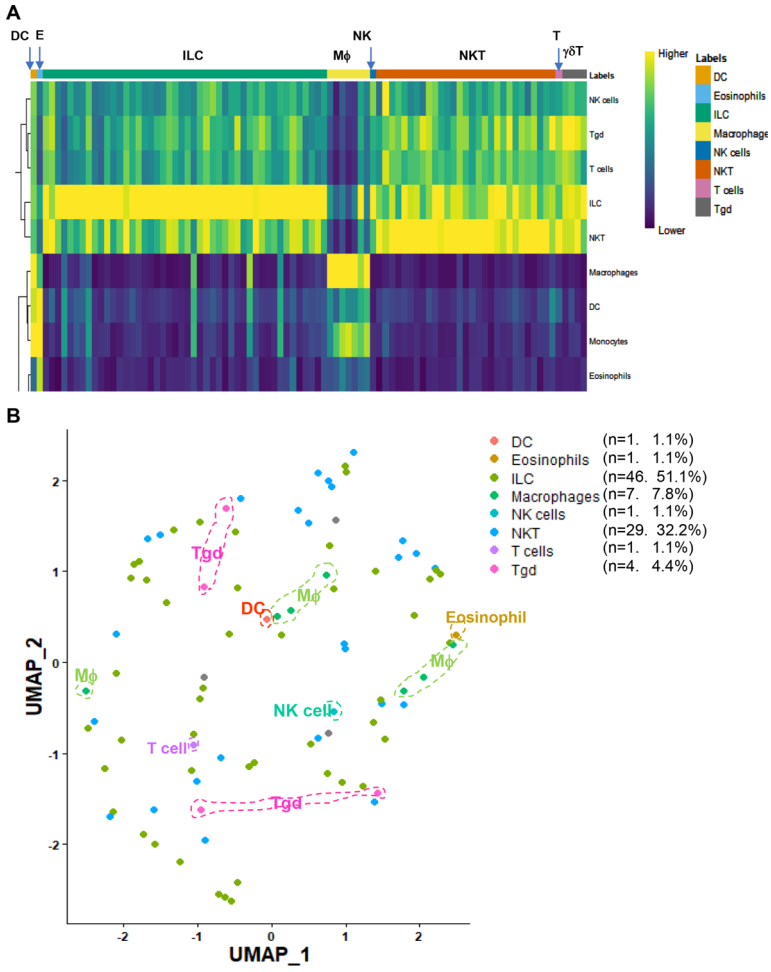


**Figure 14.**

SingleR analysis of Cluster 7 identified heterogenous innate lymphocyte populations. **A**. Heatmap of the prediction strength of Cluster 7 cells by SingleR. **B**. Unbiased re-clustering of Cluster 7 cells.

**Table 1.**

Number of sc transcriptomes obtained from total corneal cells

| | 2 mo | 6 mo | Subtotal |
|---|---|---|---|
| WT | 6915 | 7402 | 14317 |
| KO | 6526 | 5282 | 11808 |
| Subtotal | 13441 | 12684 | 26125 |

**Table 2.**

Relative representations of major cell types in mouse cornea

| | CEpiCs | CSKCs/CEndoCs | CRICs |
|---|---|---|---|
| **WT_2 mo** | 27.22% | 71.11% | 1.68% |
| **WT_6 mo** | 24.51% | 74.05% | 1.45% |
| **WT_Average** | 25.86% | 72.58% | 1.56% |
| **KO_2 mo** | 37.01% | 61.49% | 1.50% |
| **KO_6 mo** | 19.65% | 77.04% | 3.31% |
| **KO_Average** | 28.33% | 69.26% | 2.41% |

**Table 3.**

Numbers of cells sequenced in CD45+ MACS-enriched corneal cells (6 mo)

| Cluster | subtotal |
|---|---|
| WT | 1089 |
| KO | 2165 |
| subtotal | 3254 |

**Table 4.**

Sources of pooled CRICs

| Sources | Total corneal cells | | | CD45+MACS cells | Subtotal |
|---|---|---|---|---|---|
| **Age** | **2 mo** | **6 mo** | **Subtotal** | **6 mo** | |
| **WT** | 113 | 105 | 218 | 383 | 601 |
| **KO** | 97 | 174 | 271 | 1172 | 1443 |
| **Subtotal** | 210 | 279 | **489** | **1555** | **2044** |

**Table 5.**

Major myeloid cells identified by SingleR/ImmGenData

| Clusters | Number | % of all pooled CRICs | % of all corneal cells* |
|---|---|---|---|
| **Dendritic cells** | 16 | 0.78% | 0.015% |
| **Macrophages** | 1784 | 87.28% | 1.728% |
| **Microglia** | 12 | 0.59% | 0.012% |
| **Monocytes** | 26 | 1.27% | 0.025% |
| **Neutrophils** | 34 | 1.66% | 0.033% |
| **Total CRICs** | 2044 | 100.00% | 1.980% |

*: based on that, on average, CRICs account for ~1.98% of all corneal cells (Table S6).

**Table 6.**

Cell-type annotations of CRICs in adult naïve mouse cornea

| Cluster | Cell identity annotation | Predicted functional features of subtypes of Mϕ** |
|---|---|---|
| **0** | Mϕ, subtype 1 (Mϕ-1) | APP |
| **1** | Mϕ-2 | APP |
| **2** | MC, DC, Mϕ-3 | Early differentiating Mϕ |
| **3** | Mϕ-4 | M2 and M1/M2 hybrid polarity |
| **4** | Mϕ-5 | APP |
| **5** | Mϕ-6 | Early differentiating Mϕ |
| **6** | CRF * | ECM remodeling, fibrosis |
| **7** | ILC, NKT, γδT, Mϕ-7 | Innate IL-17 producers |
| **8** | CRN *, Mϕ-8 | M1 |
| **9** | Mϕ-9 | Proliferative |

* Newly identified cell types in naïve mouse cornea

** Predicted based on major features of their transcriptomes

CRF: corneal resident fibrocyte; CRN: corneal resident neutrophil; DC: dendritic cell; ILC: innate lymphoid cell; MC: monocytes; Mϕ: macrophages; NKT: natural killer T cells.